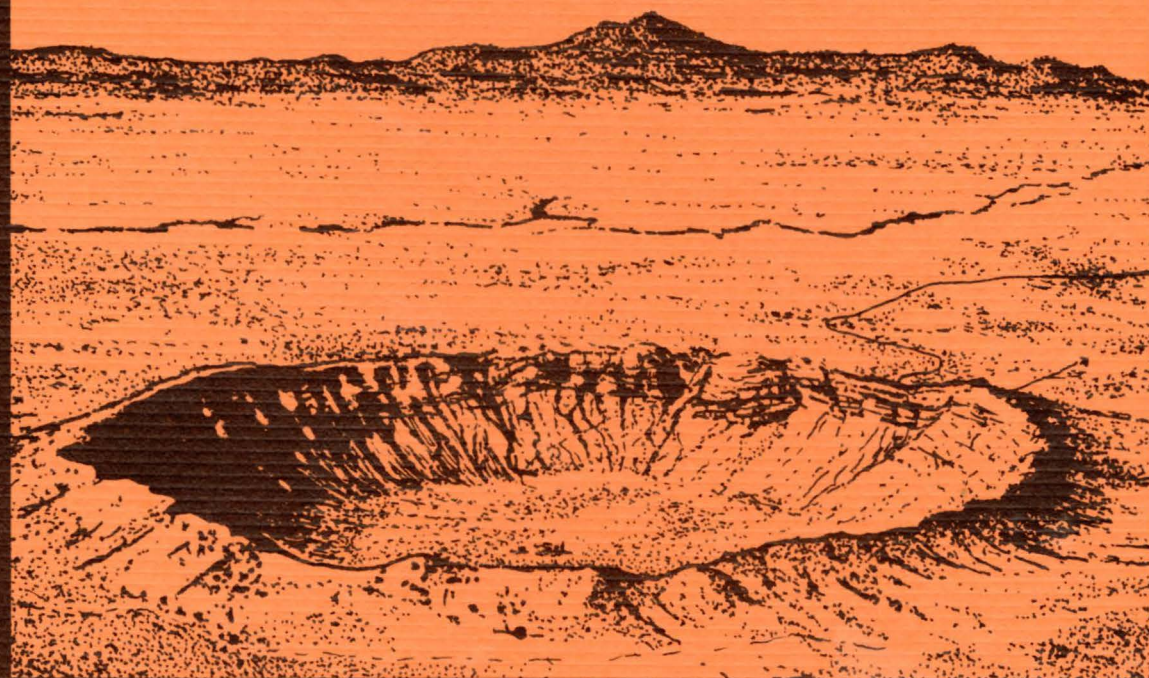# GUIDEBOOK TO THE GEOLOGY OF METEOR CRATER, ARIZONA

EUGENE M. SHOEMAKER
AND
SUSAN W. KIEFFER

CENTER FOR METEORITE STUDIES
ARIZONA STATE UNIVERSITY • TEMPE

GUIDEBOOK
TO THE
GEOLOGY OF
METEOR CRATER,
ARIZONA

Prepared by
Eugene M. Shoemaker
and
Susan W. Kieffer

for the
37th Annual Meeting
of the
Meteoritical Society
August 7, 1974

CONTENTS

SYNOPSIS OF THE GEOLOGY OF METEOR CRATER

By

Eugene M. Shoemaker

Regional Setting

Meteor Crater lies in north-central Arizona in the Canyon Diablo region of the southern part of the Colorado Plateau (Fig. 1). The climate is arid and the exposures are exceptionally good.

In the vicinity of the crater, the surface of the Plateau has very low relief and is underlain by nearly flat-lying beds of Permian and Triassic age. The crater lies near the anticlinal bend of a gentle mono-clinal fold, a type of structure characteristic of this region. The strata are broken by wide-spaced northwest-trending normal faults, gen-erally many kilometers in length but with only a few meters to about 30 meters of displacement. Two mutually perpendicular sets of vertical joints of uniform strike occur in the region of the crater. One set is subparallel to the normal faults and the other controls the trend of secondary stream courses (Fig. 1).

Basaltic cinder cones and flows of late Tertiary and Quaternary age lie at distances of about 11 to 29 km (7 to 18 miles) to the south, west, and northwest of the crater.

Pre-Quaternary Stratigraphy

Rocks exposed at Meteor Crater range from the Coconino Sandstone of Permian age to the Moenkopi Formation of Triassic age. Drill holes in and around the crater have intersected the upper part of the Supai For-mation of Pennsylvanian and Permian age, which conformably underlies the Coconino.

The Supai Formation consists of interbedded red and yellow fine-grained argillaceous sandstone and subordinate siltstone. It is more than 300 meters (1000 feet) thick in this region (Peirce, 1958, p. 84), but not more than 100 meters or so (a few hundred feet) have been penetrated by drill holes at the crater. The Coconino Sandstone (McKee, 1933) consists of about 210 to 240 meters (700 to 800 feet) of fine-grained saccharoidal, white, crossbedded sandstone. Most of the Coconino sandstone is an un-usually clean quartz sandstone; in the lower part of the formation the quartzose sandstone is interbedded with red sandstone beds of Supai
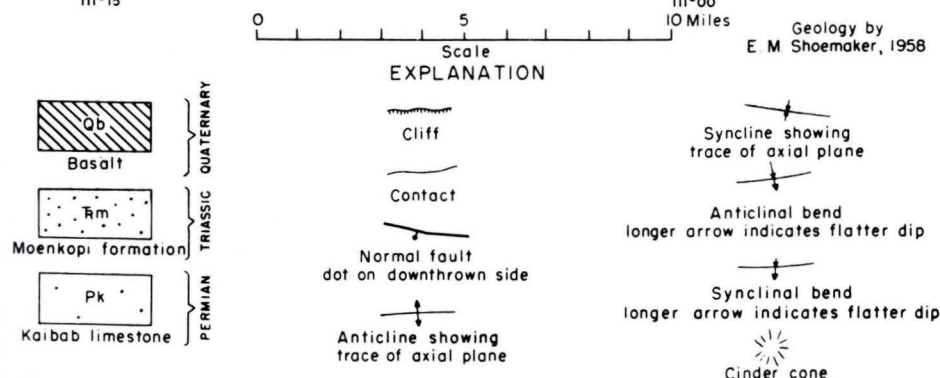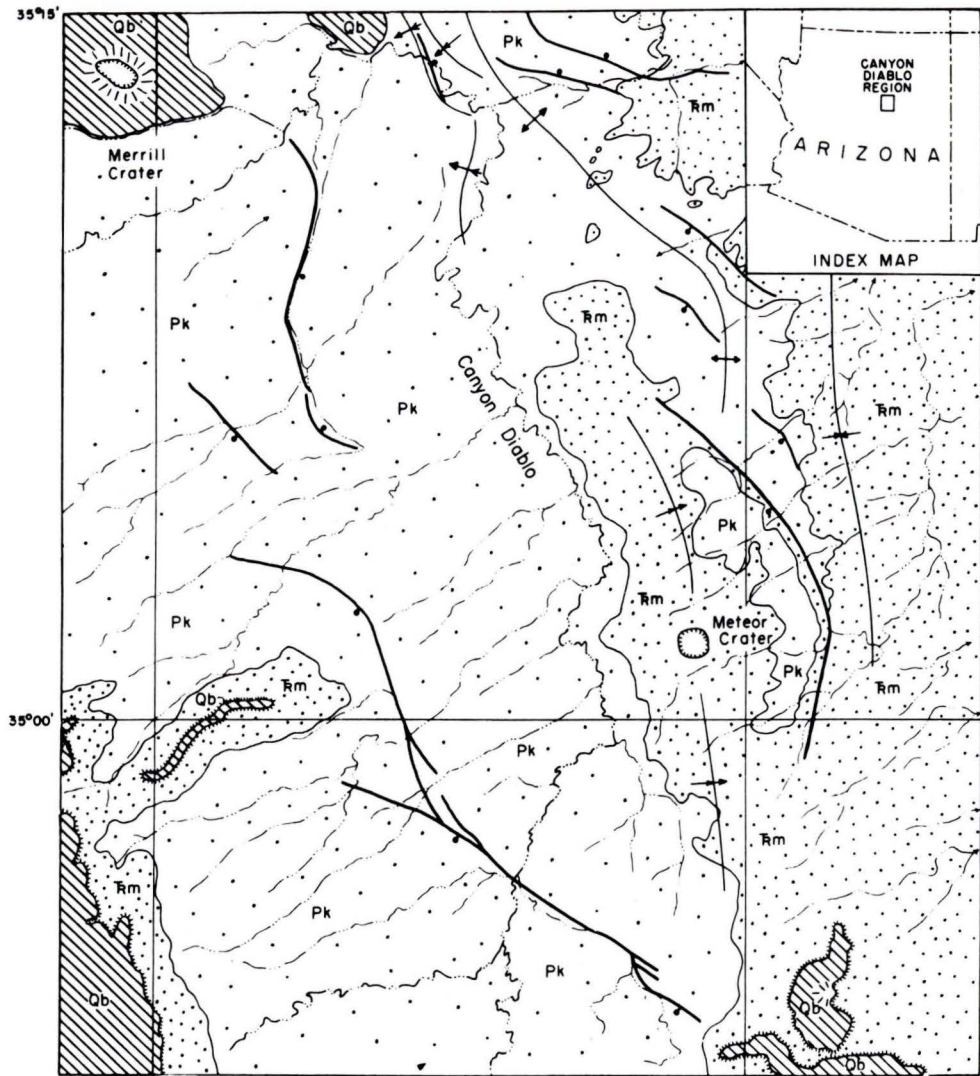
1

FIG. 1—*Sketch geologic map of Canyon Diablo region, Arizona.*

2

lithology. Only the upper part of the Coconino is exposed at the crater.
The Coconino is overlain conformably by 2.7-meter- (9-foot-) thick unit
of white to yellowish- or reddish brown, calcareous, medium- to coarse-
grained sandstone interbedded with dolomite referred to the Toroweap For-
mation of Permian age (McKee, 1938).

The Kaibab Formation of Permian age, which rests conformably on the
Toroweap Formation, includes 79.5 to 81 meters (265 to 270 feet) of
fossiliferous marine sandy dolomite, dolomitic limestone, and minor cal-
careous sandstone. Three members are recognized (McKee, 1938). The
lower two members, the Gamma and Beta Members, are chiefly massive
dense dolomite; the upper or Alpha Member is composed of well-bedded
limestone and dolomite with several continuous thin sandstone interbeds.
The Kaibab is exposed along the steep upper part of the wall of the
crater, and a large area west of Meteor Crater is a stripped surface on
the Alpha Member (Fig. 1).

In the vicinity of the crater, and to the east, beds of the Moenkopi
Formation (McKee, 1954) of Triassic age form a thin patchy veneer resting
disconformably on the Kaibab. Two members of the Moenkopi are present in
the vicinity of the crater. A 3- to 6-meter (10- to 20-foot) bed of pale
reddish-brown, very fine-grained sandstone (McKee's lower massive sand-
stone), which lies from 0.3 to 1 meter (1 to 3 feet) above the base,
constitutes the Wupatki Member. Above the Wupatki are dark, reddish-
brown fissile siltstone beds of the Moqui Member. About 9 to 15 meters
(30 to 50 feet) of Moenkopi strata are exposed in the wall of the crater.

Quaternary Stratigraphy and Structure of the Crater

Meteor Crater is a bowl-shaped depression 180 meters (600 feet) deep,
about 1.2 km (3/4 mile) in diameter, encompassed by a ridge or rim that
rises 30 to 60 meters (100 to 200 feet) above the surrounding plain. The
rim is underlain by a complex sequence of Quaternary debris and alluvium
resting on disturbed Moenkopi and Kaibab strata (Fig. 2 and Plate I).

The debris consists of unsorted angular fragments ranging from
splinters less than 1μ in size to great blocks more than 30 meters
across. Because of the striking lithologic contrast among the older for-
mations from which the debris is derived, it is possible to distinguish
and map units or layers in the debris by the lithic composition and strati-
graphic source of the component fragments.

The stratigraphically lowest debris unit of the rim is composed almost
entirely of fragments derived from the Moenkopi Formation. Within the
crater this unit rests on the edge of upturned Moenkopi beds (Fig. 3) or
very locally grades into the Moenkopi Formation; away from the crater wall
the debris rests on the eroded surface of the Moenkopi. A unit composed
of Kaibab debris rests on the Moenkopi debris. The contact is sharp
where exposed within the crater, but, at distances of 0.8 km (half a
mile) from the crater, there is slight mixing of fragments at the contact.
Patches of a third debris unit, composed of sandstone fragments from the

EXPLANATION

Recent alluvium

Pleistocene alluvium

Debris from Coconino
sandstone and
Toroweap formation

Debris from
Kaibab limestone

Debris from
Moenkopi formation

Moenkopi formation,
Wupatki member;
"Lower massive
sandstone" of McKee
(1954) unshaded

Kaibab limestone,
Alpha member
of McKee (1938)

Contact; long dashes where
approximately located, short
dashes where indefinite

Small monoclinal fold, arrow
shows downthrown side

QUATERNARY

TRIASSIC

PERMIAN

TO U.S. HIGHWAY 66

Canyon Diablo

METEOR
CRATER

T-Ranch

N 14°

Geology by
E.M. Shoemaker
1957–1958

TO CHAVES PASS

0   1   2   3 Miles

FIG. 2.—Geologic map of area around Meteor Crater, Arizona

METEOR CRATER

Qr, Recent alluvium
Qrl, Recent playa beds
Qp, Pleistocene alluvium
Qpl, Pleistocene lake beds
Qpt, Pleistocene talus

Qd, mixed debris from Coconino, Toroweap, Kaibab, and Moenkopi formations; includes lechatelierite and meteoritic material
Qct, debris from Coconino and Toroweap formations
Qk, debris from Kaibab limestone
Qm, debris from Moenkopi formation
br, breccia (includes lechatelierite and meteoritic material)

Rm, Moenkopi formation (Triassic)
Pk, Kaibab limestone (Permian)
Pct, Coconino and Toroweap formations (Permian)
PPs, Supai formation (Permian and Pennsylvanian)

NUCLEAR EXPLOSION CRATERS

TEAPOT ESS CRATER

JANGLE U CRATER

dd, dump material moved by bulldozer or power shovel
ta, scree formed in crater
al, alluvium deposited in crater
fo, fallout and throwout
br, breccia

Qrs, Recent sand
Qrg, Recent gravel
Qpb, Pleistocene paleosol, B horizon
Qp, Pleistocene alluvium

FIG. 3—*Cross sections of Meteor Crater, Arizona, and nuclear explosion craters.*

5

Coconino and Toroweap Formations, rest with sharp contact on the Kaibab debris. No fragments from the Supai Formation are represented in any of the debris.

The bedrock stratigraphy is preserved, inverted, in the debris units. Not only is the gross stratigraphy preserved, but even the relative position of fragments from different beds tends to be preserved. Thus most sandstone fragments from the basal sandstone bed of the Moenkopi Formation occur near the top of the Moenkopi debris unit, fragments from the Alpha Member of the Kaibab limestone occur at the base of the Kaibab debris unit, and brown sandstone fragments from the 3-meter- (3-foot-) thick Toroweap Formation occur just above the Kaibab debris unit.

Pleistocene and Holocene alluvium rests unconformably on all the debris units, as well as on bedrock. The Pleistocene alluvium forms a series of small, partly dissected pediments extending out from the crater rim and also occurs as isolated patches of pediment or terrace deposits on the interstream divides. It is correlated on the basis of well-developed pedocal paleosols with the Jeddito Formation of Hack (1942, pp. 48-54) of Pleistocene age (Leopold and Miller, 1954, pp. 57-60; Shoemaker, Roach, and Byers, 1962) in the Hopi Buttes region, some 80 km (50 miles) to the northeast. Holocene alluvium blankets about half the area within the first 0.8 km (half-mile) of the crater and extends along the floors of minor stream courses (Fig. 2). It includes modern alluvium and correlatives of the Tsegi and Naha Formations of Hack (1942) of Holocene age (Shoemaker, Roach, and Byers, 1962) in the Hopi Buttes region.

Both the Pleistocene and the Holocene alluvium are composed of material derived from all formations represented in the debris and also contain meteorite fragments, lechatelierite (Merrill, 1907, 1908, pp. 472-478; Rogers, 1928, pp. 82-84, and 1930), other kinds of fused rock (Nininger, 1954, 1956, pp. 117-134), and less strongly shocked rocks with coesite and stishovite (Chao, Shoemaker and Madsen, 1960; Chao and others, 1962). Oxidized meteoritic material and fragments of relatively strongly shocked Coconino Sandstone are locally abundant in the Pleistocene alluvium where it occurs fairly high on the crater rim. Unoxidized meteoritic material occurs in two principal forms: (a) large crystalline fragments composed mainly of two nickel-iron minerals, kamacite and taenite (Merrill and Tassin, 1907), and (b) minute spherical particles of nickel-iron (Tilghman, 1906, pp. 898-899, 907; Nininger, 1949, 1951a, b, pp. 80-81). The bulk of the meteoritic material distributed about the crater is apparently in the form of small particles. The total quantity of fine-grained meteoritic debris about the crater, which occurs not only in the Pleistocene and Holocene alluvium but also as lag and dispersed in colluvium, has been estimated by Rinehart (1958, p. 150) as about 12,000 tons.

Beds ranging from the Coconino Sandstone to the Moenkopi Formation are exposed in the crater walls. Low in the crater the beds dip gently outward. The dips are generally steeper close to the contact with the debris on the rim, and beds are overturned along various stretches totalling about one-third the perimeter of the crater. Along the north and east walls of the crater, the Moenkopi can locally be seen to be folded back on itself, the upper limb of the fold consisting of a flap that has been

6

rotated in places more than 180° away from the crater (Fig. 3). At one place in the southeast corner of the crater, the flap grades outward into disaggregated debris, but in most places there is a distinct break between the debris and the coherent flap.

Rocks now represented by the debris of the rim have been peeled back from the area of the crater somewhat like the petals of a flower. The axial plane of the fold in three dimensions is a flat cone, with apex downward and concentric with the crater, that intersects the crater wall. If eroded parts of the wall were restored, more overturned beds would be exposed.

The upturned and overturned strata are broken or torn by a number of small, nearly vertical faults with scissors-type displacement. A majority of these tears are parallel with the northwesterly regional joint set, and a subordinate number are parallel with the northeasterly set. Regional jointing has controlled the shape of the crater, which is somewhat squarish in outline; the diagonals of the "square" coincide with the trend of the two main sets of joints. The largest tears occur in the "corners" of the crater. In the northeast corner of the crater a torn end of the overturned flap of the east wall forms a projection suspended in debris. A few normal faults, concentric with the crater wall, occur on the southwest side. A number of small thrust faults occur on the north and west sides of the crater. Relative displacement of the lower plate is invariably away from the center of the crater. Crushed rock is locally present along all types of faults; it has been designated *authigenic breccia* in Plate 1, to distinguish it from another type of breccia under the crater floor.

The floor of the crater is underlain by Quaternary strata, debris, and breccia. Pleistocene talus mantles the lowest parts of the crater walls and grades into Pleistocene alluvium along the floor. The Pleistocene alluvium, in turn, interfingers with a series of lake beds about 30 meters (100 feet thick) toward the center of the crater. Up to 1.6 meters (6 feet) of Holocene alluvium and playa beds rest unconformably on the Pleistocene. Where exposed in shafts, the lowermost Pleistocene lake beds contain chunks of pumiceous, frothy lechatelierite.

A layer of mixed debris underlies the Pleistocene talus and lake beds and rests on bedrock and on breccia. This layer is composed of fragments derived from all formations intersected by the crater and includes much strongly shocked rock and oxidized meteoritic material. The material from all the different sources is thoroughly mixed. Where intersected by a shaft in the crater floor, it is about 10.5 meters (35 feet) thick and almost perfectly massive, but exhibits a distinct grading, from coarse to fine, from base to top. The average grain size, about 2 cm, is much less than in the debris units of the rim or in the underlying breccia; the coarsest fragments at the base rarely exceeding 0.3 meter (1 foot) in diameter. I believe that this unit was formed by fallout of debris thrown to great height. It has not been recognized outside the crater, probably because it has been entirely eroded away. Its constituents have been partly redeposited in the Pleistocene and Holocene alluvium.

Where exposed at the surface, the breccia underlying the mixed
debris is composed chiefly of large blocks of Kaibab, but the breccia
exposed in shafts under the central crater floor is made up chiefly of
shattered and twisted blocks of Coconino. Extensive drilling conducted
by Barringer (1906, 1910, 1914) and his associates (Tilghman, 1906)
has shown that, at a depth of 100 to 200 meters (300 to 650 feet),
much finely crushed sandstone and some fused and other strongly rock
and meteoritic material are present. Some drill cuttings from about 180
meters (600 feet) depth contain fairly abundant meteoritic material. In
cuttings examined by the writer the meteoritic material is chiefly in the
form of fine spherules dispersed in glass, similar to the impactite
described by Nininger (1954) and by Spencer (1933, pp. 394-399) from the
Wabar and Henbury meteorite craters. Cores of ordinary siltstone and
sandstone of the Supai were obtained at depths of 210 meters (700 feet)
and deeper. The lateral dimensions of the breccia are not known because
the drilling was concentrated in the center of the crater. Some of
the meteorite-bearing or *allogenic* breccia was evidently encountered in
a hole drilled from 1920 to 1922 on the south rim of the crater (Barringer,
1924). (See log of hole in Hager, 1953, pp. 840-841.)

Mechanism of Crater Formation

Nearly all the major structural features of Meteor Crater, Arizona,
are reproduced in a crater in the alluvium of Yucca Flat, Nevada, formed
by the underground explosion of a nuclear device. The Teapot Ess crater
(Fig. 3), about 90 meters (300 feet) across and originally about 30 meters
(100 feet) deep, was produced in 1955 by a 1.2 kiloton device detonated
at a depth of 20 meters (67 feet) below the surface (Johnson, 1959, p. 10).
Beds of alluvium exposed in the rim are peeled back in an overturned syn-
cline, just as the bedrock is peeled back at Meteor Crater. The upper
limb of the fold is overlain by and locally passes outward into debris that
roughly preserves, inverted, the original alluvial stratigraphy. Shock-
formed glass and other strongly shocked materials, some containing coesite,
are present in the uppermost part of the debris. A thin layer of debris
formed by fallout or fall-back is also present in the crater. The floor
and lower walls of the crater are underlain by a thick lens of breccia
containing mixed fragments of alluvium and dispersed glass. Some of the
fragments are strongly sheared and compressed. The breccia was formed by
complex movement of material within the crater; locally, the original
bedding of the alluvium is roughly preserved in the breccia.

A crater with the structure of Teapot Ess crater is formed chiefly
by two mechanisms, which operate in succession. First, the alluvium,
as it is engulfed by a compressional shock caused by the explosion,
is accelerated in all directions radially outward from the detonated
device, and an expanding cavity is formed underground. When the shock
reaches the free surface of the ground, it is reflected as a tensional
wave. Momentum is trapped in the material above the cavity, and it con-
tinues to move up and outward, individual fragments following ballistic
trajectories. Kinetic energy is also imparted to the fragments from ex-
panding gases in the cavity. Ejected fragments close to the crater maintain

their approximate relative positions, inverted during flight. Along low-velocity trajectories, their range is largely a function of the angle at which they are thrown out, which in turn varies continuously with their original position relative to the nuclear device. The margin of the crater is determined primarily by the radial distance, in plan, at which the reflected tensional wave is just strong enough to lift and separate the alluvium. The position at which this occurs is just inside of and concentric with the hinge of the overturned flap, i.e., the intersection of the axial plane of overturning with the surface of the ground. The reflected tensional wave starts a fracture at the surface but does not appreciably change the momentum of most of the material thrown out. Beds are sheared off along a roughly conical surface that starts at the surface slightly inside the hinge and is propagated downward to join tangentially the lower part of the hole expanded behind the shock front. Material brecciated by very strong shock initially has the form of a roughly spherical shell around the hole, but most of the upper hemisphere is thrown out, and the lower hemisphere is sheared out in the form of a concavo-convex lens. Overturning of the beds in the upper crater wall may be looked on as drag along the conical shear zone.

It is essential that the shock originate deeper than a certain minimum distance below the surface, relative to the total energy released, in order to produce the overturned syncline in the rim. A crater formed near the Teapot Ess crater by a nuclear device of the same yield, but detonated at 5.4 meters (18 feet) depth rather than 20 meters (67 feet) (Fig. 3, Jangle U crater), has an anticline under the rim, not a syncline. An explosion at such a depth (shallow relative to the yield of the device) produces a crater more through radial expansion of the cavity behind the shock and less by ejection of material than in the case of Teapot Ess crater. The greatest expansion of the hole occurs at the surface because of upward relief of stress at the free surface, which manifests itself in concentric anticlinal buckling.

The structure of Meteor Crater would be produced by a very strong shock originating about at the level of the present crater floor (120 meters (400 feet) below the original surface. A minimum scaled depth of penetration of the meteorite or of a major part of the energy associated with the meteorite is indicated by the overturned synclinal structure of the rim. A closer estimate of the depth for the apparent origin of the shock can be obtained from the base of the breccia under the crater floor by scaling from Teapot Ess crater. Some limits may also be set on the mechanics of impact by the fact that the shock was strong enough to fuse Coconino Sandstone, at a depth of some 90 meters (300 feet) or more below the surface, and that part of the meteorite itself was fused by shock on impact, as shown by the dispersal of spherical particles of meteoritic material in some of the fused rock.

Not all meteorite craters exhibit overturned synclines in the rim, as at Meteor Crater, which indicates that the scaled depth of penetration on impact is not always so great. The rim of the main meteorite crater at Odessa, Texas, for example, is underlain by an anticline similar to that

of the Jangle U crater (compare with Hardy, 1953; Sellards and
Evans, 1941.

The reconstructed sequence of events in the formation of Meteor
Crater, based on theoretical analysis (Shoemaker, 1960), is illustrated
in Figure 4. The crater was formed by impact of meteoritic iron bolide
about 30 meters (100 feet) across. On the basis of scaling from the
Sedan Crater in Nevada, the energy released by impact was 4 to 5 mega-
tons TNT equivalent. This event occurred a few tens of thousands of
years ago, as shown by the mid-Wisconsin age of the oldest sedimentary
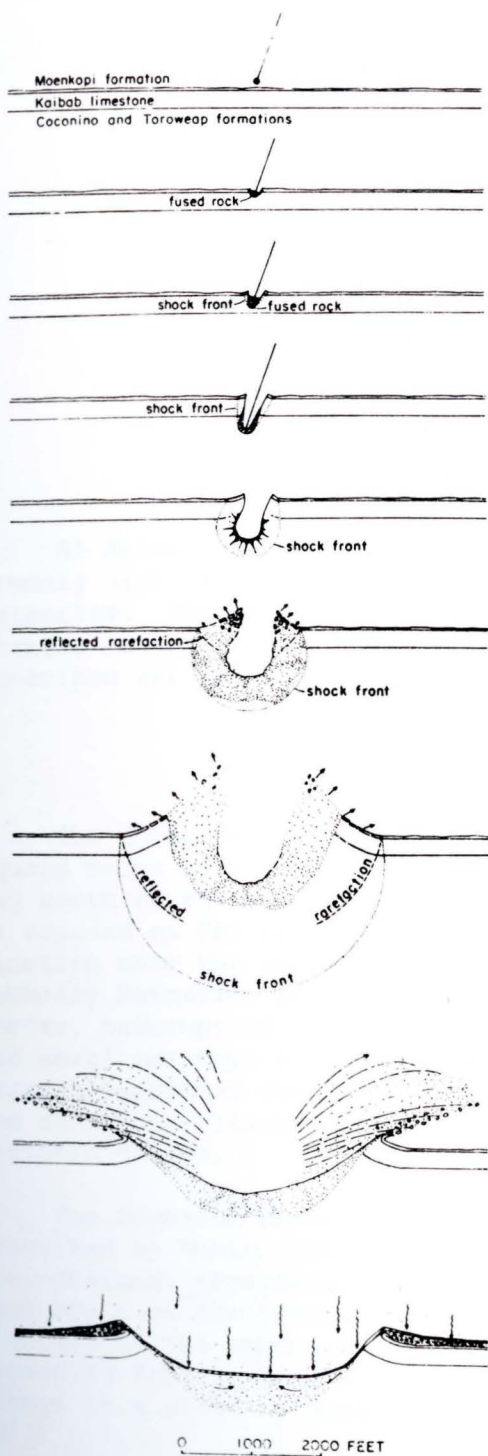deposits on the rim and in the interior of the crater.

Moenkopi formation
Kaibab limestone
Coconino and Toroweap formations

fused rock

shock front — fused rock

shock front —

~shock front

reflected rarefaction —

~shock front

reflected   rarefaction

shock   front

0   1000   2000 FEET

1. Meteorite approaches ground at 15 km/sec.

2. Meteorite enters ground, compressing and fusing rocks ahead and flattening by compression and by lateral flow. Shock into meteorite reaches back side of meteorite.

3. Rarefaction wave is reflected back through meteorite, and meteorite is decompressed, but still moves at about 5 km/sec into ground. Most of energy has been transferred to compressed fused rock ahead of meteorite.

4. Compressed slug of fused rock and trailing meteorite are deflected laterally along the path of penetration. Meteorite becomes liner of transient cavity.

5. Shock propagates away from cavity, cavity expands, and fused and strongly shocked rock and meteoritic material are shot out in the moving mass behind the shock front.

6. Shell of breccia with mixed fragments and dispersed fused rock and meteoritic material is formed around cavity. Shock is reflected as rarefaction wave from surface of ground and momentum is trapped in material above cavity.

7. Shock and reflected rarefaction reach limit at which beds will be overturned. Material behind rarefaction is thrown out along ballistic trajectories.

8. Fragments thrown out of crater maintain approximate relative positions except for material thrown to great height. Shell of breccia with mixed meteoritic material and fused rock is sheared out along walls of crater; upper part of mixed breccia is ejected.

9. Fragments thrown out along low trajectories land and become stacked in an order inverted from the order in which they were ejected. Mixed breccia along walls of crater slumps back toward center of crater. Fragments thrown to great height shower down to form layer of mixed debris.

FIG. 4—*Diagrammatic sketches showing sequence of events in formation of Meteor Crater, Arizona.*

SHOCK METAMORPHISM OF

THE COCONINO SANDSTONE AT METEOR CRATER

By

Susan W. Kieffer

At Meteor Crater the Coconino Sandstone was metamorphosed by extremely high pressures and temperatures associated with the impact of the meteorite. The unshocked sandstone and the textural and mineralogical changes recognized in shocked samples are described below. The features described are illustrated in Figures 5 and 6.

Unshocked Sandstone

The Coconino Sandstone (named by Darton, 1910) underlies 32,000 square miles of the Colorado Plateau province in northern Arizona, extending south to the Mogollon cliffs and west to the Grand Wash cliffs. It is exposed as far east as Holbrook, Arizona, and thins to apparent extinction near the Utah border, but probably grades laterally into the DeChelly Formation in the north (Baker and Reeside, 1929). At Meteor Crater, outcrops of Coconino Sandstone are best seen on the east wall, but small outcrops also occur on the north, west, and south walls. The nearest exposures outside of the crater are 24 km (15 miles) to the south. The sandstone attains a maximum thickness of 330 m (1000 feet) at its southern extent.

The Coconino Sandstone, as exposed in the Grand Canyon, was first described by Noble (1914). He described wedge-shaped units of pale buff, fine-grained, crossbedded sandstone whose distinctive features are the huge scale of the crossbedding, the massive appearance and the uniform fineness of the component grains of sand. The wedge-shaped units often exceed 40 feet in length and 100 feet in height. The dip of the bedding planes in a southern direction is commonly 15° to 25°, or exceptionally, 30°.

The origin and mode of transport of the Coconino sands has long been a subject of controversy. There is general agreement that the beds dip to the south (Reiche, 1938) implying that the direction of transport was from the north. Schuchert (1918), on the basis of ripple marks found in the Coconino in one place at the Hermit Trail, Grand Canyon, postulated that the sands comprised a large delta of continental deposits laid down under constant, but probably local, sheets of fresh water. Read (1950, 1961) interpreted the Coconino sands as beach and nearshore
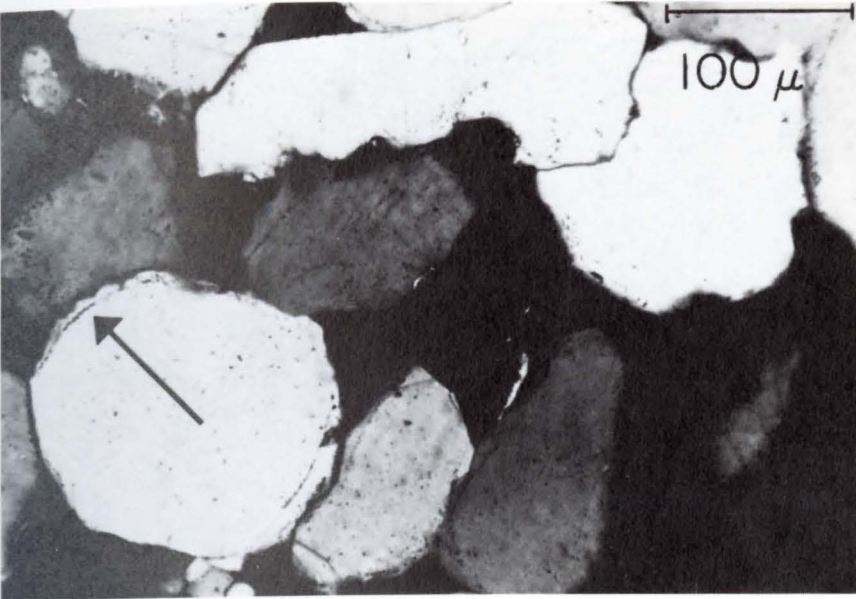
12

Figure 5a.
Unshocked Coconino.
Boundaries between
detrital grains and re-
crystallized quartz
cement are commonly
marked by lines of
vesicles (arrow).
Crossed polarizers.

Figure 5b.
Class 1b shocked
Coconino. Brittle
fractures and fine
fragments fill
collapsed pores.
Arrows indicate
apparent direction
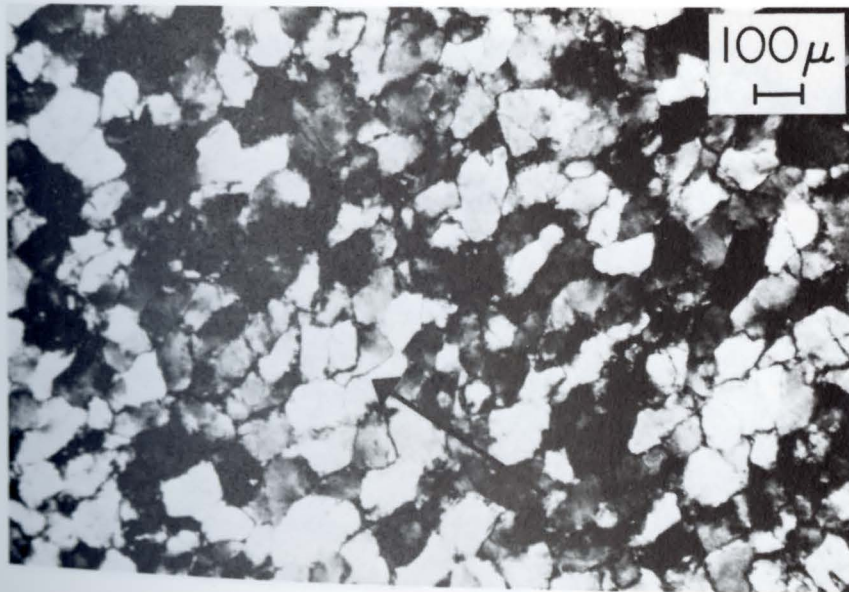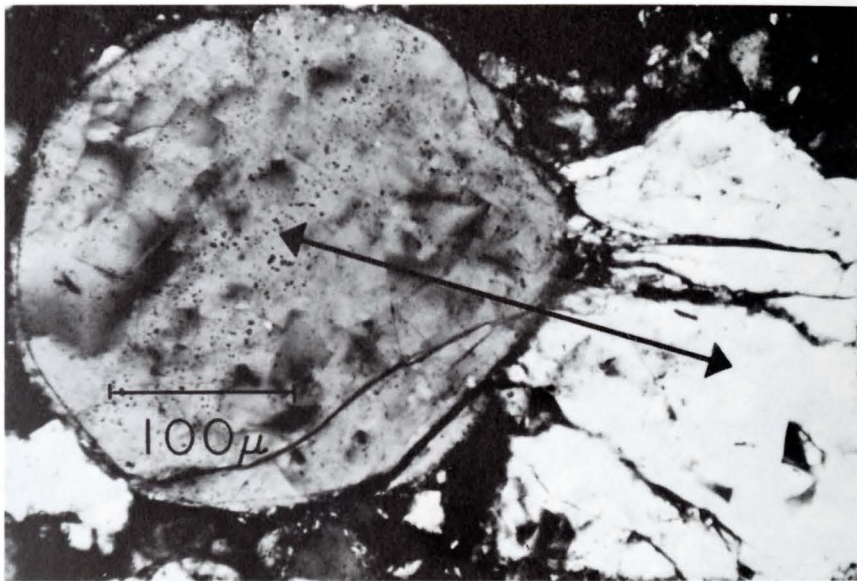of shock compression.
Crossed polarizers.

Figure 5c.
Class 2 shocked
Coconino. Quartz grains
deformed into inter-
locking shapes (arrow),
resembling pieces of a
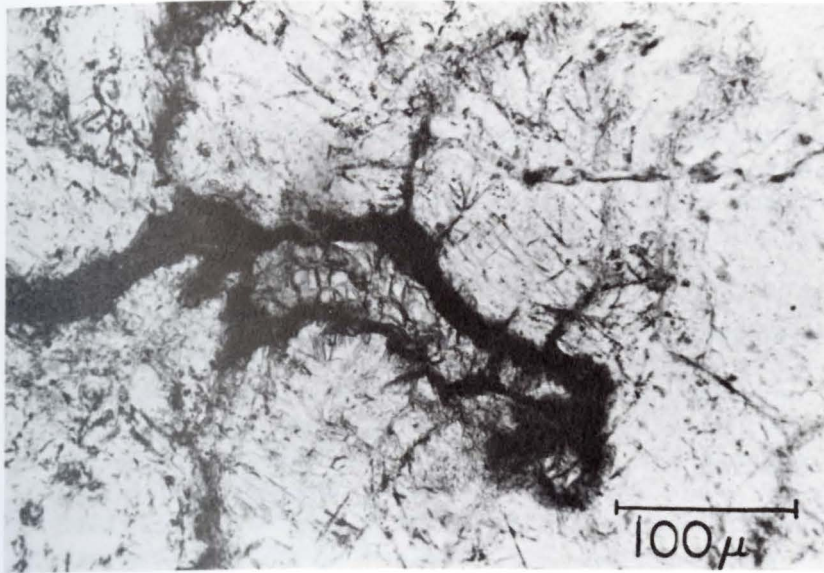jigsaw puzzle. Crossed
polarizers.

Figure 6a.
Class 3 shocked Coconino.
A core of crypto-
crystalline coesite in
the center of the photo-
micrograph is surrounded
by an opaque rim and
fractured quartz grains.
Thin veins of symplektic
material pervade the
quartz grains. Plane
polarized light.

Figure 6b.
Class 4 shocked Coconino.
The central dark area
is isotropic and con-
tains vesicular glass.
It is surrounded by a
thin opaque rim contain-
ing coesite and glass.
The (white) quartz
grains are generally
highly shocked and
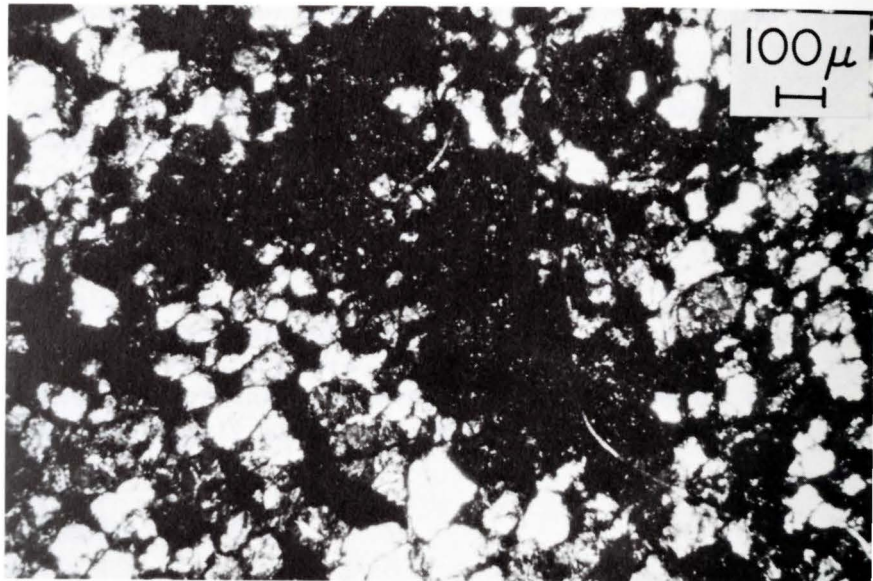contain veins of
symplektic material.
Crossed polarizers.

Figure 6c.
Class 5 shocked Coconino.
Vesicular lechatelierite
which has flowed, show-
ing elongated vesicles
and schlieren. Plane
polarized light.

14

deposits. Reiche (1938), McKee (1934), Matthes (quoted by McKee, 1934) and Opdyke and Runcorn (1960) cite the preservation of vertebrate tracks on the crossbedded surfaces, wind ripples and the great extent of the homogeneous quartz sand as evidence that the sand was transported and deposited by wind.

The upper part of the Coconino as exposed at Meteor Crater is a pale buff, white or pink crossbedded sandstone. The coarseness of the cross-bedding causes a massive appearance in outcrop. Occasional fragments of Coconino show red stains on weathered surfaces. In hand specimen and thin section, two textures are evident: (1) massive (laminations, if they exist, are several centimeters thick) and, (2) laminated (parallel laminae are 1/2 to 2 mm thick). The main constituents of the sandstone are quartz (>95%), sericite and clay minerals (<5%), heavy minerals (<2%), rock fragments (<2%), feldspars (<1%), and traces of hematite and geothite. Recrystallized quartz is the primary cement in the Coconino at Meteor Crater.

The detrital quartz grains (Fig. 5a) are well rounded and, in the massive rocks, have longest dimensions between 0.1 mm and 3.9 mm, with a mean length of 0.2 mm. The porosity, as determined in thin section, varies from 9% to 18% in the massive rocks. The pores are extremely complex and irregular and are distributed nonuniformly throughout the rock. Variation in porosity on both a large scale and small scale (locally within a hand specimen or thin section) had a significant effect on the nature of the shock wave passing through the material. The existence of at least a small amount of water in the pores at the time of crater for-mation is inferred from the presence of lake sediments in the bottom of the crater and from the texture of the highly shocked rocks.

Shocked Sandstone

Shock metamorphosed Coconino Sandstone was first recognized at Meteor Crater by Barringer (1905), Tilghman (1905) and Fairchild (1906). These investigators recognized three main types of shock metamorphosed specimens: crushed and pulverized sandstone; compressed rock with a higher density than the original sandstone and a slaty structure (called Variety A by Barringer); and, cellular pumiceous lechatelierite which floats on water (called Variety B). In the Variety B rocks, Rogers (1928) recognized grains of silica glass which retained the structure of the sandstone from which they formed and which he called "paramorphs of lechatelierite after quartz." Chao (1967) and von Engelhardt and Stöffler (1968) have recognized glass with the same property and refer to it as diaplectic or thetomorphic glass.

Coesite (Chao, Shoemaker and Madsen, 1960) and stishovite (Chao, and others, 1962) were first discovered as naturally occurring minerals at Meteor Crater in the Variety A rocks and as minor constituents in the Variety B rocks. Coesite is the stable phase of SiO_2 between pressures of approximately 30 kb and 75 kb and stishovite is the stable phase above these pressures.

Shocked specimens of Coconino Sandstone distributed in and around the Crater can be divided into five classes briefly described below (Kieffer, 1970, 1971). The classes are defined on the basis of the amount of quartz present in the rocks. The amounts of coesite, stishovite, and glass vary systemmatically with decreasing quartz content (Fig. 7). Rock fabric and texture are strongly correlated with this classification. The classes are:

Class 1. Weakly shocked rocks containing no high-pressure phases and 95 percent or more quartz. Subclass A: with petrographically observable remnant porosity; Subclass B: without petrographically observable remnant porosity.

Class 2. Moderately shocked rocks containing 80 to 95 percent quartz. They typically have 2 to 5 percent coesite, 3 to 10 percent glass, and no detectable stishovite.

Class 3. Moderately shocked rocks containing 40 to 80 percent quartz. These rocks typically contain 18 to 32 percent coesite, trace amounts (<1%) of stishovite, and up to 20 percent glass.

Class 4. Strongly shocked rocks containing 15 to 45 percent quartz. They typically have 10 to 30 percent coesite, 20 to 75 percent glass, and no detectable stishovite.

Class 5. Very strongly shocked rocks that contain 0 to 15 percent quartz. These rocks may have 0 to 5 percent coesite, 0 to 100 percent glass, and no detectable stishovite.

The rocks were metamorphosed to these varying degrees by a shock wave of complex structure. The shock wave consisted of a relatively sharp rise to peak pressure, the shock front, and a slower decay to ambient pressure, the rarefaction. Shock waves are propagated through porous rocks like the Coconino by grain-to-grain collisions across pores. Such collisions cause a series of shocks and rarefactions within each grain during the initial compression. Successive rarefactions and shocks take the grains to progressively lower peak pressures and higher temperatures until an equilibrium state is approached. Equilibrium conditions in pressure are reached only after a few microseconds to tens of microseconds. Shear deformation, simple oblique impacts and complex jetting phenomena complicate the shock structure and contribute to additional pressure and temperature inhomogeneities.

High pressure and/or high-temperature phases in shocked Coconino sandstone samples occur in regions which were systematically related to initial geometry, to pressure and temperature gradients in the shock, and to the presence of interstitial water. Locally high pressures enduring for microseconds and high temperatures enduring for milliseconds controlled the phases of SiO_2 that formed and survived in the rocks. Collapsing pore walls became local hot spots into which initial deposition of energy was focused.
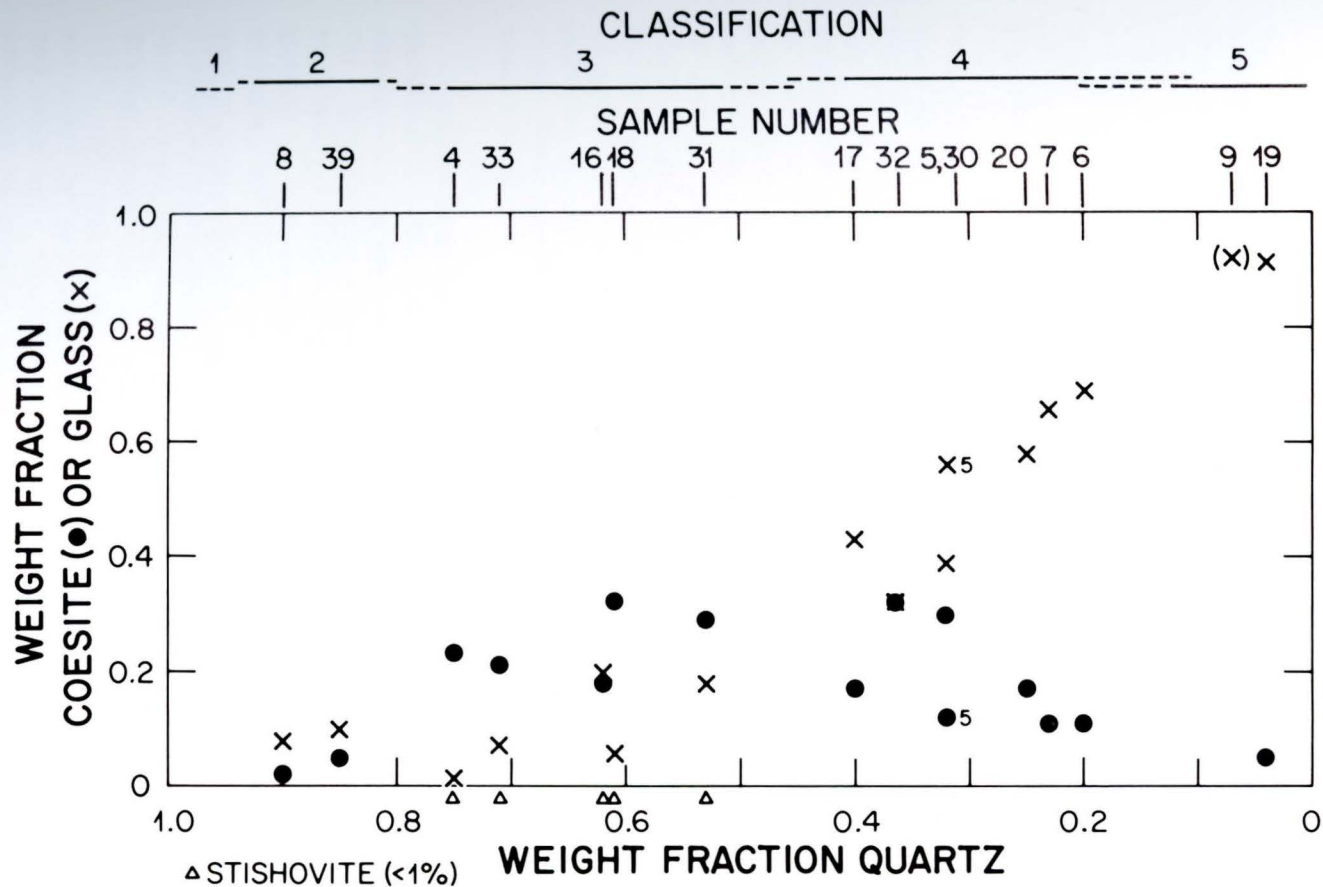
CLASSIFICATION

Figure 7. Abundance of coesite (o) and glass (x) in shocked Coconino Sandstone as a function of quartz content. Rocks in which stishovite was detected (greater than 0.25% and less than 1% by weight) are indicated by a triangle. Limiting quartz contents of the five classes of shocked rocks are shown at the top of the figure. Sample numbers of rocks examined by x-ray diffraction are also shown at the top of the graph.

Rocks of the lowest class of shock metamorphism resemble unshocked Coconino Sandstone in hand specimen, Class 1A, or are finely fractured, friable white rocks, Class 1B, (Figure 5b). The quartz grains are fractured, but no high-pressure phases are detectable by x-ray methods (that is, the weight fraction of high-pressure phases of grain size larger than 1,000 Å is less than 0.5%). Voids which existed in the unshocked rocks are filled with myriads of small chips. These small fragments were produced by brittle fracturing of quartz grains, frequently along crystallographic directions. The fractures were produced as neighboring grains collided in the shock wave.

Class 2 rocks are well indurated and dense, and are usually white in hand specimen. Some specimens display thin (<0.5 mm) parallel fractures. The quartz grains retain their initial size, but are deformed to interlock with one another like pieces of a jigsaw puzzle (Figure 5c). The grains are elongated and aligned in a direction interpreted to be tangential to the shock front. This deformation was accomplished principally by intense fracturing and crushing along narrow rims on grain boundaries. Small amounts of coesite nucleated and grew in the crushed fraction on the edges of quartz grains. Observations of the grain boundary regions with a transmission electron microscope (Kieffer, Phakey and Christie, 1974) show that direct quartz to coesite transitions occurred and that some of the coesite is partially inverted to glass resembling thetomorphic glass. A comparison of the composition of these rocks with laboratory equation of state data suggests that average shock pressures in these rocks were less than 100 kb.

Class 3 rocks are well indurated, dense and often show a platy structure. The high-pressure phases, coesite and stishovite, occur in regions which may be easily identified in thin section (Figure 6a): (1) symplektic regions which appear gold or brown in thin section because they are partially opaque, owing to the presence of small coesite grains embedded in quartz boundaries; (2) opaque regions, containing intimate mixtures of quartz, coesite, stishovite and glass and; (3) cryptocrystalline coesite cores, which are ellipsoidal regions of 50 to 200 μm dimension containing cryptocrystalline coesite. Electron microscopy reveals that the cores are composed of an equigranular mosaic of coesite. Triple junctions of grain boundaries commonly subtend angles close to 120°, indicating an "equilibrated" texture. Such a texture is common in annealed or recrystallized metals and indicates that the coesite nucleated and grew to a "mature" polycrystalline structure from a high-temperature, probably amorphous, phase. The texture of these cores and the initial geometry of pores in the unshocked Coconino has led Kieffer, Phakey and Christie (1974) to postulate that the cores originated as molten jets which were injected into collapsing pores during the passage of the shock wave. Such jets are formed when particles impact obliquely if particle velocities are greater than ∼1-2 km/sec and impact angles are greater than ∼30°. As shock pressures decayed in the rarefaction, the jets cooled and coesite nucleated and grew from the high temperature amorphous material. In the quartz surrounding the cores, coesite formed directly from quartz; this coesite is now seen in the symplektic and opaque regions and generally

occurs as 1 μm tabular twinned crystals, many of which are partially inverted to glass. Stishovite also formed directly from quartz and is now found in the opaque regions.

The electron microscope observations also revealed the presence of a fine froth in the regions containing high-pressure phases in the class 3 rocks. This froth is not resolvable by optical methods but is probably the main cause of opacity in the opaque regions. The froth is vesicular at a scale of tens of angstroms. The vesicles are irregular in shape and are surrounded by thin walls of amorphous silica. The froth occupies fractures and cracks in quartz, coesite and stishovite and was therefore deposited after the high-pressure phases had formed in the shock event. Kieffer, Phakey and Christie (1974) have suggested that the froth formed as silica precipitated from a cooling water vapor saturated in silica. Silica was dissolved from quartz and coesite grains as water, initially in the pores, was heated by the shock. Under conditions near the critical end point of the univariant equilibrium melting curve of the SiO_2-H_2O system (9.7 kb, 1080°C), water may dissolve up to 70% by weight of silica. Sudden cooling of such a hot, silica-saturated mixture during the rarefaction is believed to have produced the froth as silica precipitated from the mixture. A model for the behavior of water under shock conditions and comparison of the rock compositions with laboratory equation of state data suggests that the class 3 rocks formed at pressures in the range 100 to 250 kb.

Class 4 (Figure 6b) and Class 5 (Figure 6c) rocks are vesicular and are usually distinguishable by their elongated, aligned fractures and vesicles. The fractures may be lined with calcite. In thin section it may be seen that vesicular glass in Class 4 rocks occurs in cores up to 3 mm in longest dimension. These cores are surrounded by opaque rims which contain microcrystalline coesite and glass. The cores of glass were formed as jets of molten silica were squirted into collapsing pores. As in the Class 3 rocks, coesite nucleated and grew in the cores of the Class 4 rocks. Grains up to 50 μm diameter have been observed in the vesicular glass with the electron microscope. Nearly all of the coesite inverted to glass during the rarefaction. The vesicles were formed as water,which had been incorporated into the silica melt at pressures above the critical end point of the SiO_2-H_2O system,exsolved upon release to low pressure. In the glassy core regions these vesicles coalesced to give spherical or elliptical vesicles as large as 5 millimeters diameter. In the opaque regions the small vesicles coalesced in glass along the boundaries of coesite grains to form the fractures observed in hand specimens of Class 4 rocks. Class 5 rocks formed by this same process and represent extreme conditions of pressure and temperature such that nearly all material has been converted to glass. Comparison of this inferred behavior of the silica-water system with laboratory equation of state data suggests that pressures in excess of 200 kb were present in the Class 4 and 5 rocks.

ROAD GUIDE FROM FLAGSTAFF TO METEOR CRATER TURNOFF

By

Eugene M. Shoemaker, Susan W. Kieffer, and Robert L. Sutton

———————

Kilometers
(Miles)

0.0
(0.0)

Butler Street interchange, U.S. Interstate Highway 40 (I-40), heading east toward Meteor Crater and Winslow. Just north of U.S. Route 66 in Flagstaff, at 9:00 below the horizon, is Switzer Mesa, which is capped by Pliocene basalt flows dated at 5.80 ± 0.34 m.y. (Damon and others, 1974). The relatively straight margins of Switzer Mesa suggest that basaltic lava once flowed down a graben valley and that subsequent erosion produced the present "reverse topography." This filled graben is one of many straight-walled valleys and escarpments formed in the pre Plio-Pleistocene deposits by pervasive normal faulting. Cropping out below the protective lava cap of Switzer Mesa is part of the lower Wupatki Member of the Moenkopi Formation of Early Triassic age (McKee, 1951).

San Francisco Mountain, including Humphreys Peak, and Elden Mountain are visible at 10 and 11 o'clock, respectively, on the left. San Francisco Mountain, a largely andesitic stratovolcano, probably attained a total eruptive elevation of more than ~4500 m (15,000 feet). The volcano may have been modified by either summit collapse or explosive eruption. More recent fluvial and glacial erosion have also modified the form of the volcano. Humphreys Peak, elevation 3851 m (12,633 feet), is the highest mountain in Arizona. Elden Mountain (2835 m; 9299 feet) is a dacite dome, complex in detail because part of it (north) appears to be laccolithic, tilting and exposing pre-Kaibab Paleozoic rocks as old as Devonian, while another part (the south end, visible from the road) was extrusive (Kluth and Kluth, 1974). Large viscous flow lobes with marked jointing can be seen from the highway on the south and east sides of the mountain.

1.0
(0.6)

The road cut exposes the top of the Alpha Member of the Kaibab Formation of Permian age (McKee, 1938). The top of the Kaibab is an ancient karst surface. The upper 20 to 30 meters

(65 to 100 feet) of the Kaibab Formation appear to have been modified by solution.

1.6
(1.0)

The road crosses a southeast-trending escarpment bordering a small valley ("park") which is probably a graben.

4.7
(2.9)

Route 89 north toward Page and Grand Canyon exists here. Continue west on I-40.

5.3
(3.3)

Proceed slowly! About 100 meters ahead of you, a fault-line scarp is visible. The downthrown block is on the west and forms the small depression which you are traversing. On the left at 9:00 o'clock is Sheep Hill, a cinder cone of the Tappan age-group (Moore and others, 1974). As you approach the fault-line scarp, a quick glance to the rear at about 5:00 o'clock will reveal a basalt flow in the depression below I-40. This flow emanated from the base of Sheep Hill. The east margin of this depression is sometimes occupied by an ephemeral lake, Bill Fill Lake.

5.5
(3.4)

In the escarpment directly east of Big Fill Lake and in the road cut, the jumbled beds of the karst horizon of the Alpha Member of the Kaibab Formation is again exposed. A distinctive red bed sequence may be seen below the top of the Kaibab; this unit thins toward the east and is not present at Meteor Crater. The entire Kaibab Formation pinches out 30 miles beyond Meteor Crater.

5.6
(3.5)

Many quarries are dug into the cinder cones, such as Sheep Hill (at 9:00 o'clock), Wildcat Hill (11:00 o'clock), and Turkey Hill. The cinders are used in road metal and in cinder blocks. There are more than 400 cinder cones in the San Francisco volcanic field.

9.7
(6.0)

Turn off to Walnut Canyon National Monument.

10.0
(6.2)

The red beds in the Alpha Kaibab Formation are again exposed in the road cut north of eastbound I-40.

13.6
(8.4)

Cosnino road exit.

14.5
(9.0)

Normal fault, downthrown to the west.

15.6
(9.7)

From this section of the road, the view to the south is of a stripped surface developed on top of the Kaibab Formation. Topography in this area accurately reflects the bedrock structure, except where it is moderately dissected by gullies.

Kilometers (Miles)	
16.1 (10.0)	At about 8 o'clock, below the horizon, Sunset Crater is visible as a bright-rimmed cinder cone, devoid of vegetation. It lies just to the right of, and below, O'Leary Peak. The most recent eruption in the volcanic field occurred in 1064 A.D. at Sunset Crater. The date is based on dendrochronology (Smiley, 1958).
18.0 (11.2)	Along the highway good exposures of thin grey beds within the Alpha Member of the Kaibab Formation are visible beneath 1 to 3 m of the jumbled rocks in the karst horizon. The Kaibab here is mostly silty dolomite and dolomitic sandstone with some chert. Marine fossils (brachiopods such as Derbya; productids; cephalopods; invertebrates; a few fish teeth) are abundant in many beds.
18.2 (11.3)	At 10:30 o'clock is a large cinder quarry (the Darling pit) at Cinder Mountain, owned by the Santa Fe Railroad.
18.9 (11.7)	Walnut Canyon
19.3 (12.0)	A lava flow of the Tappan age-group (Moore and others, 1974), is visible in the road cut. For the next 2.5 miles a cinder blanket of variable thickness covers the land surface. The cinders probably came from four cinder cones just south of the highway.
20.0 (12.4)	Winona exit. The basaltic cinder cone on the right has a rootless lava flow on its northwestern flank. This cone is probably the source of the lava flow at mile 12.0. A last view of Sunset Crater silhouetted in front of O'Leary Peak may be obtained by looking back to the left (about 8 o'clock?).
21.9 (13.6)	The road drops back to the stripped surface on the Kaibab, thinly strewn with cinders. To the left, just beyond the Santa Fe railroad tracks, is the margin of a basaltic lava flow.
23.5 (14.6)	Looking ahead, the road rises over a gentle anticline, reflected as a swell on the stripped surface on top of the Kaibab Formation.
24.1 (15.0)	Three miles to the north at 9:30 o'clock, Piper Crater, a basaltic cinder cone, is superposed on the south side of Rattlesnake Crater, an older maar-type vent. Merrill Crater is east of Piper Crater at 10 o'clock.
27.5 (17.1)	Merriam Crater is located in the distance at 9:00 o'clock.
29.5 (18.3)	The small cinder cone at 3:00 o'clock is the nearest Quaternary volcanic feature to Meteor Crater.

30.6
(19.0)

The eastward gradient of the highway steepens noticeably as it comes over the crest of the anticline mentioned at mile 14.6. From here, the road descends into Padre Canyon. The Hopi Buttes volcanic field can be seen in the distance (about 80 km; 50 mi) at 10 to 11 o'clock, across the Little Colorado River valley). On the skyline to the right is Anderson Mesa, capped by basalt flows dated at 6.2 ± 1.2 m.y. (Damon, 1965).

32.0
(19.9)

Padre Canyon and Twin Arrows Trading Post.

34.1
(21.2)

As one looks out across the broad stripped surface on the Kaibab, it should be kept in mind that in this region of the Colorado Plateau, the topography reflects the structures beneath. A broad anticline is visible in the distance ahead. Normal faults which have been crossed are controlled by a regional pattern of jointing. Two orthogonal sets of joints which trend predominantly northeast and northwest are parallel to important regional structures in this part of the Colorado Plateau (Colton, 1936).

36.9
(22.9)

The long ridge between about 2 and 3 o'clock is an irregular basalt capped ridge which extends toward Meteor Crater and will be seen end on from road to Meteor Crater.

40.8
(25.3)

For the next 2 miles the highway traverses an anticline where an oil test well was drilled to Precambrian strata in 1962, about half a mile north of the highway (NE¼ NW¼ sec. 12, T. 20 N., R. 11 E.). The well was converted for watering stock. Following are subsurface thicknesses of Paleozoic formations penetrated by this well (Peirce and Scurlock, 1972, p. 159):

	Feet	Meters
Kaibab (Permian).	283	86.3
Coconino (Permian).	890	271.3
Supai (Permo-Pennsylvanian)	1370	417.7
Naco (Pennsylvanian).	515	157.0
Molas (Pennsylvanian)	12	3.7
Redwall-Zones A, B, C (Mississippian.	110	33.5
Martin (Devonian)	380	115.8
Precambrian, depth	3560	1085.4
Precambrian, elevation	2175	663.1
Total depth of well	3630	1106.7

The Toroweap Formation, a marine unit between the Kaibab and the Coconino Formations in the Grand Canyon, was not recognized in this well as it is readily confused with the Coconino (McKee, 1938). Approximately the lower 73 m (240 ft) of Coconino in this well are correlated with the DeChelly Sandstone, which thickens toward the Defiance Plateau (Peirce and Scurlock, 1972).

Kilometers
(Miles)

41.1 (25.5)	The escarpment crossed by the road is a fault-line scarp on the flank of the anticline. The bedrock is downthrown to the east and exhibits reverse drag.
42.4 (25.7)	Crest of anticline.
42.8 (27.2)	A good view is obtained here of the rim of Meteor Crater in the distance at 1:00 o'clock. The Hopi Buttes volcanic field has become more prominent on the left horizon at about 11 o'clock.
46.8 (29.1)	The road rises over the crest of another anticline. East and West Sunset Buttes are visible in the distance to the right of Meteor Crater.
47.6 (29.6)	A fault-line scarp bounding the drainage at 1:30 to 3:00 at a distance of about one half mile is along a normal fault downthrown to the west.
49.4 (30.7)	Canyon Diablo
50.5 (31.4)	Weathered outcrops of massive sandstone beds in the Wupatki Member of the Moenkopi sandstone (Triassic) form characteristic knobby or biscuit-like outcrops just above the Kaibab limestone.
55.1 (34.2)	Meteor Crater exit from I-40.

ROAD GUIDE FROM METEOR CRATER TURNOFF

TO PARKING LOT AT METEOR CRATER

By

Eugene M. Shoemaker and Susan W. Kieffer

Kilometers
(Miles)

0.0   Begin at turnoff from I-40 to Meteor Crater.
(0.0)

1.0   Road Stop 1.--The first stop is at Indian Country Road
(0.6)   intersection. To the east may be seen an abandoned stone build-
ing (Fig. 8) located just north of the old alignment of U.S.
Highway 66. This building once housed H. H. Nininger's
meteorite collection. It was operated as a museum, open to
the public at a fee, where visitors heard lectures by Nininger
and could study the collection and purchase specimens. The
operation of this museum was the source of Nininger's liveli-
hood for many years. Visitors could climb the stone tower
and look off to the north to get a view of Meteor Crater with-
out deviating from their route on Highway 66.

The museum is built just above a low escarpment which trends
northwest-southeast and can be traced by eye for a distance of
about two miles. The escarpment is along a small normal fault
which offsets the lower beds of the Moenkopi at this place. The
throw on the fault is about 9 meters (30 feet). On the upthrown
side may be seen outcrops of the Lower Massive Sandstone unit
of the Wupatki Member of the Moenkopi Formation, which are the
lowermost beds of the Moenkopi at this place. Erosional remnants
of the Lower Massive Sandstone form a line of small knobs trend-
ing off to the southeast. About 3 meters (10 feet) of siltstone
and very fine sandstone of the Moqui Member of the Moenkopi
Formation are preserved locally above the Lower Massive Sandstone.
Nininger's old museum is built of pieces of Moenkopi sandstone
from both the Wupatki and Moqui Members. Some of these pieces
are beautifully ripplemarked (Fig. 9).

A water well, 100 meters (300 feet) away, at 11 o'clock,
brings water up from the middle of the Coconino Sandstone at a
depth of 200 meters (600 feet). The Coconino Sandstone is the

25

Figure 8.
Road Stop 1.
*H. H. Nininger's
old museum
(photographed here
from the northeast)*.

Figure 9.
*Detail of wall of Nininger's
old museum, showing ripple-
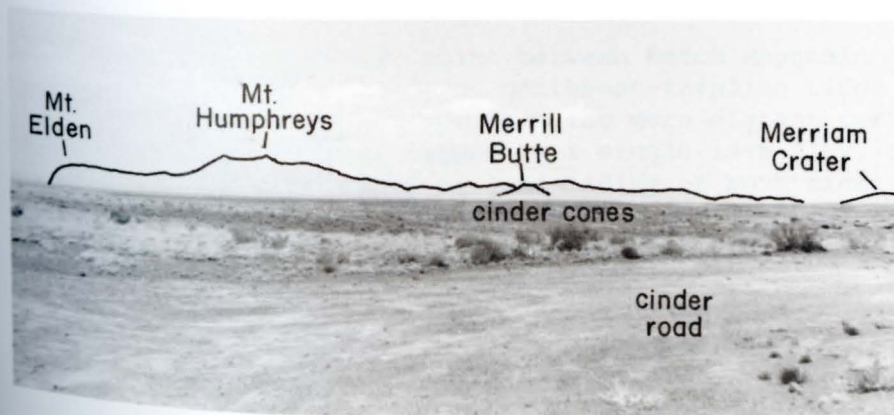marked stones from the Moenkopi
Formation.*

Mt.
Elden
Mt.
Humphreys
Merrill
Butte
Merriam
Crater
cinder cones
cinder
road

Figure 10.
Road Stop 2.
*View of the San
Francisco volcanic
field.*

26

principal aquifer in this part of northern Arizona. Here the
water table slopes gently to the north, in the same direction as
the average regional dip of the beds. Meteor Crater is lo-
cated on the southern flank of the Black Mesa basin; the beds
dip generally about one degree to the northeast.

1.8
(1.1)
The road drops into a shallow valley where Wupatki sandstone
is well exposed.

3.2
(2.0)
The road drops to the level of the Moenkopi-Kaibab con-
tact. A few scattered blocks of Kaibab Limestone may be seen
to the side of the road.

4.7
(2.9)
Road Stop 2.--Here the road comes over the crest of a rise,
and the visitor obrains a first good overall view of the crater
rim. At this point, the road is on the Moqui Member of the
Moenkopi, about 5 meters (15 feet) above the base of the Moqui
Member.

To the left and behind the rim of Meteor Crater may be seen
the lava-capped mesas known as East Sunset Butte and West Sunset
Butte. Both buttes are capped by basalt, which rests on the
Chinle Formation of Upper Triassic age. The flanks of the buttes
visible from the vantage point along the road are mantled with
landslide debris which supports a pygmy forest of pinyon and
juniper. In places along the flanks of the buttes, not visible
from this point, a complete section of the Moenkopi Formation and
a partial section of the Chinle Formation are exposed. Three
cinder cones are visible on the buttes which mark the vents from
which the basaltic lavas were erupted.

To the right of Meteor Crater, from about 12 o'clock to about
3 o'clock, the skyline is formed by basalt-capped mesas of the
Mormon Mountain volcanic field. The basalts in this field are
Miocene and Pliocene in age. One of the basalts capping Anderson
Mesa, at 3 o'clock, is dated at 6.2 ± 1.2 m.y. (Damon, 1965). The
two highest points visible in the volcanic field are Hutch
Mountain, at about 1:30, and Mormon Mountain, at about 2 o'clock.

The high point between Hutch Mountain and Mormon Mountain is
the end of a long, northeast-trending ridge that extends directly
toward the viewer from the more distant part of the volcanic field.
The ridge is capped by a single lava flow, most of which has now
been destroyed by landsliding on both sides of the ridge. Red
beds of the Chinle Formation and Moenkopi Formation may be seen
exposed in parts of the landslide blocks on the near end of the
ridge.

Between 3 o'clock and 5 o'clock lie the volcanoes of the San
Francisco volcanic field (Fig. 10). The largest volcano is San

Francisco Mountain.   A circle of peaks surround the eroded core
of this volcano, the highest of which is Mt. Humphreys.   At
3851 meters (12,633 feet), Mt. Humphreys is the highest point
in Arizona.   The San Francisco stratovolcano is composed mainly
of andesite lava flows and ashes.   Rhyolites and dacites occur
as domes perched on the flank of the older stratovolcano.   The
largest of these domes forms Mount Elden, which is the prominent
toe extending to the left of the main mountains.   Domes which
have been dated range in age from 2.71 ± 0.13 m.y. to 0.212 ±
0.011 m.y. (Damon and others, 1974).

To the right of the San Francisco peaks is an extensive
field of Pleistocene basaltic cinder cones.   This is the main
locus of basaltic activity, at the present time, in the San
Francisco volcanic field.   The youngest cinder cone in this field,
not visible from this vantage point, is Sunset Crater, which has
been dated by dendrochronological methods at 1064 A.D. (Smiley,
1958).   The nearest prominent reddish colored cinder cone is
Merrill Butte, which lies about 27 km (17 miles) airline distance.
At the extreme right of the volcanic field is a large symmetrical
cinder cone called Merriam Crater.   The cinders on the side road,
extending to the west, and also used as aggregate in the asphalt
capping of the Meteor Crater road, have been excavated from
basaltic cinder cones.

7.7   <u>Road Stop 3 (at junction of Bar-T-Bar Ranch Road)</u>.--Low
(4.8)   buttes on each side of the road are formed by beds of the Moqui
Member of the Moenkopi Formation.   An excavation around the flank
of the butte, on the right side of the road (Fig. 11), is a fossil
quarry excavated by the University of California.   Materials re-
covered from this quarry include an extensive collection of foot-
prints and fossils of ganoid fishes and amphibians.   On the basis
of regional studies of the stratigraphy of the Moenkopi Formation
and on fossils obtained from this and other nearby quarries, the
beds at this horizon can be placed near the base of the Middle
Triassic.   The fossils were found in freshwater dolomite and
siltstone beds in the floor of the quarry.   These beds are no
longer exposed.

8.8   <u>Road Stop 4</u>.--This stop is just beyond a broad curve in the
(5.5)   road at a point where road heads nearly due east.   To the north
of the road, at 9 o'clock, the skyline is formed by a ridge of
siltstone and sandstone of the Moqui Member of the Moenkopi
(Fig. 12).   The south slope of the ridge is mantled with late
Pleistocene colluvium containing abundant fragments of sandy dolomite
from the Kaibab Formation.   These fragments have been derived by re-
working of a blanket of ejecta that surrounds the crater.   At one
time this ejecta blanket extended beyond the ridge of Moenkopi, but
the more distant parts of that blanket have now been eroded away
during the time elapsed since the crater was formed.   The col-

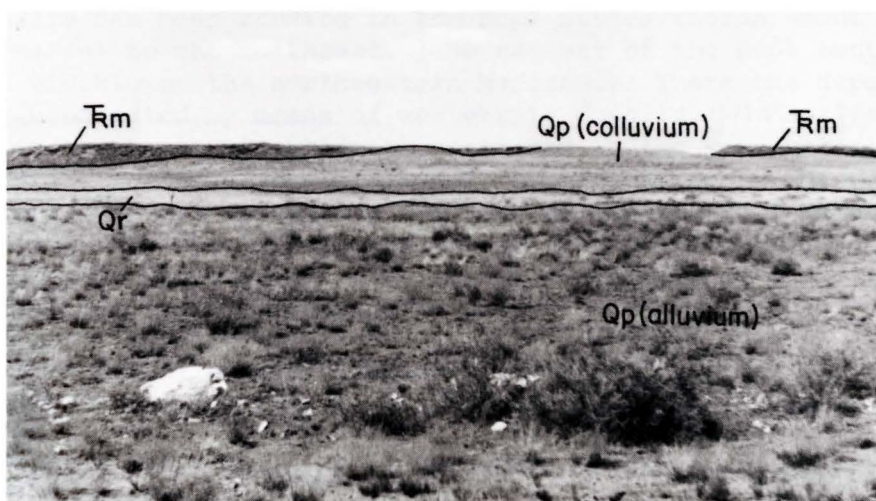*Figure 11.* *Road Stop 3.* *Filled-in fossil quarry excavated by The University of California.*

Figure 12. *Road Stop 4.* *View to north.* *The Moqui Member of the Moenkopi Formation, Ҡm, crops out on the skyline.* *Late Pleistocene colluvium, Qp (colluvium),containing fragments of dolomite from the Kaibab Formation mantles the slope extending toward the observer.* *In the drainage in the middle of the view, Holocene alluvium, Qr, overlies the colluvium.* *The surface rising from the drainage toward the observer is a late Pleistocene alluvial deposit, Qp (alluvium).*

Kilometers
    (Miles)

luvium extends to the south into a shallow drainage where it is
overlain by a thin deposit of Holocene alluvium. The outer
eroded edge of the ejecta blanket lies essentially at this
position, and is concealed beneath late Pleistocene and
Holocene alluvial deposits.

The difference in elevation between the crest of the
Moenkopi ridge and the lowest outcrop in the ejecta blanket, near
the drainage, provides a minimum estimate of the relief on the
precrater surface. It is clear that the ridge of Moenkopi is
an erosional feature that predated the crater and had a pre-
crater relief of at least 15 meters (50 feet).

On the near side of the drainage is a surface that climbs
gradually toward the crater rim and which is underlain by late
Pleistocene alluvium. The road bed is built on this alluvial
unit. The age of this and other alluvial deposits at Meteor
Crater has been determined by correlation of pedocal paleosols de-
veloped on them. A well-defined sequence of Pleistocene and Holocene
deposits has been studied in the Hopi Buttes region, about 80 km
(50 miles) to the northeast. (The nearest of the Hopi Buttes are
just visible on the northeastern horizon.) There the deposits
have been dated by means of vertebrate fossils, C-14 analysis,
and on the basis of artifacts contained in the youngest alluvial
units. A well-developed paleosol, corresponding to the youngest
Pleistocene soil in the Hopi Buttes, is exposed in a shallow
borrow pit in the alluvium 50 meters (170 feet) to the south of the
road. This Pleistocene alluvium rests directly on the preserved
part of the ejecta blanket.

The ejecta blanket surrounding Meteor Crater is stratified
and can be divided into three distinct mappable units:

1)   a unit composed of fragments of the Moenkopi Formation
     at the base,

2)   a unit composed of fragmental debris from the Kaibab
     Formation, and

3)   a unit composed of fragments of the Coconino Sandstone
     at the top.

Exposures of the Kaibab debris unit can be seen between 10 o'clock
and 3 o'clock. At 3 o'clock the Kaibab debris rises high on the
crater rim. Low mounds with large, light-colored blocks, lying
100 to 300 meters (300 to 1000 feet) from this vantage point, be-
tween 10 o'clock and about 1 o'clock, are exposures of the Kaibab
debris unit that protrude through the surrounding Pleistocene
alluvium. This part of the crater rim is essentially a stripped

surface on the top of the Kaibab debris unit. The gently hummocky topography of the rim reflects the original configuration of the contact between the Kaibab debris unit and the overlying Coconino debris unit, which has been largely stripped away.

At 2 o'clock, on the horizon, is the chimney of a building now destroyed by fire (Fig. 13). This building was the headquarters for the exploration activity of the old Standard Iron Company and the latter-day Barringer Crater Company. During the 1930's and 1940's, after exploration had ceased, the building also served as a visitor center and a small museum for the public visiting the crater. This building is constructed on a high-level pediment surface that is cut into the rim units of the crater. The pediment is capped by relatively coarse alluvial and colluvial debris derived from still higher parts of the rim. The pediment can be traced as a cut surface between about 1:30 and 3 o'clock. The easternmost edge of the pediment lies just to the left of a powder magazine, which has been dug in a brilliant white deposit beneath the pediment gravels. This white deposit is a remnant of the Coconino Sandstone debris unit, which is preserved in a pocket beneath the pediment gravels.

The difference in elevation between the highest recognizable pediment on the crater rim and the upper edges of the latest Pleistocene alluvial deposits at this locality provide a minimum estimate for the amount of dissection of the rim by erosion that has occurred since the crater has formed. On the northeast flank of the crater rim this difference is about 12 meters (40 feet). The total amount of degradation of the rim is, of course, substantially greater than this. A conservative but realistic estimate of the total reduction in rim elevation by erosion would be 15 to 20 m (50 to 75 feet). In places the rim crest may have been eroded down as much as 30 m (100 feet). In most places the Coconino debris unit has been entirely stripped away.

9.3
(5.8)

Road Stop 5 (by trailer instruction sign and just beyond road to water well).--At approximately 1 o'clock may be seen a tongue-shaped mass of light-colored rocks, extending to the crest of the crater rim (Fig. 14). This mass is a remnant of the Coconino Sandstone debris layer preserved in a depression on the top of the Kaibab debris layer. Kaibab debris underlies the grassy slopes surrounding the Coconino debris remnant. A water well at 7:30 extends slightly below the water table at a depth of about 200 meters (600 feet). This well provides the water for the museum and the visitor center on the crater rim and for the residences of the museum staff.

9.7
(6.0)

Road Stop 6 (in lower parking lot).--Exposures in cuts at the southeast corner of parking lot provide an excellent introduction into the nature of the rim debris units. A part of the
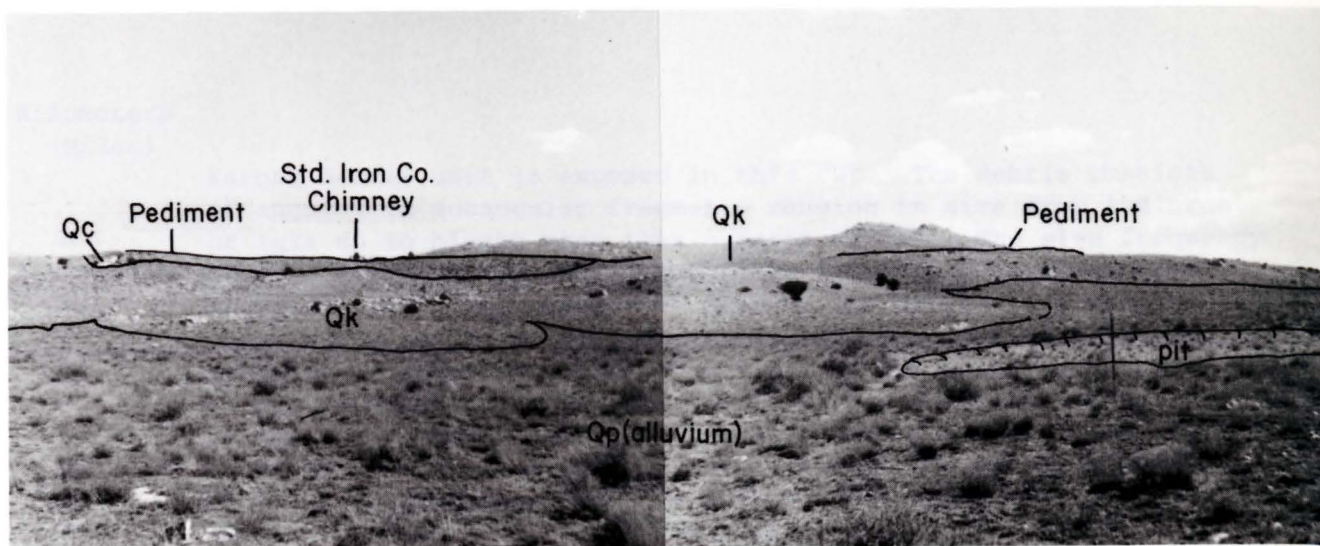
Figure 13. *Road Stop 4*. *View to south. The late Pleistocene alluvium, Qp (alluvium),extends up the flank of the crater. Outcrops of the Kaibab debris unit, Qk, form low mounds. The old Standard Iron Company building is on a high-level pediment surface. Coconino Sandstone debris, Qc, is visible at the powder magazine at the left. The shallow borrow pit to the right exposes a Pleistocene paleosol.*

Figure 14. *Road Stop 5*. *View to south. Tongue-shaped deposit of light-colored rocks is a remnant of the Coconino Sandstone debris unit, Qc, pre-served in a depression on top of the Kaibab debris unit, Qk.*

32

Kaibab debris unit is exposed in this cut. The debris consists
of angular to subangular fragments ranging in size from 1 micron
or less up to blocks more than a meter across. The size frequency
distribution of this material follows a rather well-known frag-
mentation law. The cumulative mass of the debris is a simple
power function of the particle size. The exponent of this power
function is such that about 50 percent of the total mass falls
in the largest three phi intervals. As one examines the debris
in the cut, about 50 percent of the volume of the material con-
sists of easily recognized fairly coarse blocks set in a matrix
of finer crushed material. In general, the fines are only
recognizable in fresh exposures such as this. The effect of
weathering is to wash away the fines, leaving the surface mantled
with the coarser debris. When seen on a natural outcrop, the debris
unit appears to be composed almost entirely of the coarser blocks.

GUIDE TO THE ASTRONAUT TRAIL AT

METEOR CRATER

By

Eugene M. Shoemaker and Susan W. Kieffer

The Astronaut Trail begins at the Museum on the south rim of the crater. Proceed 24 meters (80 feet) down the paved walk to trail station 1.

Trail Station 1 (located at junction of Moon Mountain side trail).--
At this point on the rim, the trail descends across the base of the debris units and into upturned bedrock (Fig. 15). The uppermost bedrock unit exposed here is sandstone of the Wupatki Member of the Moenkopi Formation. The uppermost beds of the Wupatki sandstone are peeled up sharply and locally are overturned along a line of Kaibab blocks that have been placed to mark out the limits of the Moon Mountain trail. Just upslope from the Moon Mountain sign, bedrock Moenkopi sandstone passes gradationally into overturned Moenkopi debris. The axis of overturning lies 0.3 meter (1 foot) upslope from the sign.

The top of the Moenkopi debris unit lies about 6 meters (20 feet) farther upslope. A large block of yellow vuggy sandy dolomite about 2 meters across, which has rolled slightly out of place, is one of the basal fragments in the overlying Kaibab debris unit. Pieces of Moenkopi debris can be seen around the base of the block. The contact of the Moenkopi debris with Kaibab debris unit continues to the east from this block, rising gradually as the rim crest rises to the east.

A careful study of the internal stratification of the Kaibab debris unit shows that the pieces of the Kaibab Formation occur in inverted relative stratigraphic position to one another. Pieces from the upper part of the Kaibab Formation are found near the base of the Kaibab debris layer, and pieces from the lowermost part of the Kaibab Formation occur near the top of the Kaibab debris layer. The yellow dolomite block is derived from an eight-foot bed of dolomite near the top of the Alpha Member of the Kaibab Formation. The bed from which the block is derived will be seen near the trail at the next stop.

About 12 meters (40 feet) farther along the Astronaut Trail, where steps cross the sandstone of the Wupatki Member of the Moenkopi, a narrow bleached zone may be observed in the sandstone. This bleached zone is controlled by a joint cutting the sandstone. Limonite stains on the surface

34

Figure 15. Trail Station 1. *Upturned bedrock of the uppermost beds of the Wupatki Sandstone of the Moenkopi Formation, ℞m, passes gradationally into Moenkopi debris, Qm.*

Figure 16. Trail Station 2. *Outcrop of the uppermost unit of the Alpha Member of the Kaibab Formation under Brunton compass.*

of the joint suggest that, initially, sulfides were crystallized on the joint; these sulfides subsequently have been oxidized, after erosion brought the beds above the water table. Subsurface exploration of similar bleached zones in the Morrison Formation on the Colorado Plateau indicate that the bleaching is a result of reduction of hematite in the red beds to iron sulfides.

Extensive bleaching has taken place in the sandstone of the Wupatki prior to the formation of the crater. In some places, the entire member has been bleached. Thus, the color observed on the outcrops of the Wupatki may be either red, which is the original unaltered color, or buff, which is the color of the altered zones. The contact between the red and buff zones is usually sharp, and may be followed as a wavy line in places across the entire sandstone unit. Along the Astronaut Trail, both red and buff Wupatki sandstone will be seen, both in the bedrock units and in the debris. Don't be fooled by these differences in color.

Proceed 24 meters (80 feet) in a direction south 75° east from base of stairway.

Trail Station 2.--At this point the Astronaut Trail drops into the uppermost unit of the Alpha Member of the Kaibab Formation (Fig. 16). This unit is a dolomitic sandstone with very irregular to chaotic bedding. It contains many individual sandstone and sandy dolomite clasts. Here it is about 1 meter thick and crops out as a ragged knob. The unit has been formed by partial solution or leaching of the uppermost Kaibab beds over a fairly long interval of time extending from the Middle Permian to the Middle Triassic. Essentially this unit is a residual deposit developed on a karst surface during this time interval. Directly downslope from the leached unit is a sequence of medium-bedded sandy dolomite, sandstone, and minor limestone about 4 meters (13 feet) thick. Below this lies the yellow, vuggy dolomite bed which is the parent bed for the yellow dolomite block seen in the debris at Station 1. This yellow dolomite is a prominent marker bed which can be traced almost continuously around the crater rim.

Looking across the crater at the south wall, a completely exposed section of the Kaibab Formation can be seen (Fig. 17). The basal unit of the Kaibab Formation, the Gamma Member, forms a relatively smooth bluff, just to the right of a zig-zag trail that ascends the crater wall along a broad talus apron. In a gully to the right of the trail, a small cave is eroded out in the Toroweap Formation just beneath the Kaibab; the bluff of the Gamma Member overhangs the slope below. The Gamma Member consists of medium- to thick-bedded sandy dolomite. It forms a relatively prominent cliff or ledge at the base of the Kaibab around most of the crater wall. A dark stain coats much of the smooth bluff of the Gamma Member on the south wall and forms drapery-like markings on the lower part of the bluff.

The broken slope above the bluff is underlain by the Beta Member of the Kaibab. The Beta Member extends to the base of a nearly vertical cliff just above a long stain of red drilling mud on the south crater wall. This member consists of very faintly bedded to massive white sandy dolomite.

Figure 17.
Trail Station 2.
View of south crater
wall. Units shown in-
clude Toroweap For-
mation, Pt, the Gamma,
Beta, and Alpha
Members of the Kaibab
Formation, Pk(γ),
Pk(β), and Pk (α),
and the Wupatki and
Moqui Members of the
Moenkopi Formation.
Position of white
marker sandstone,
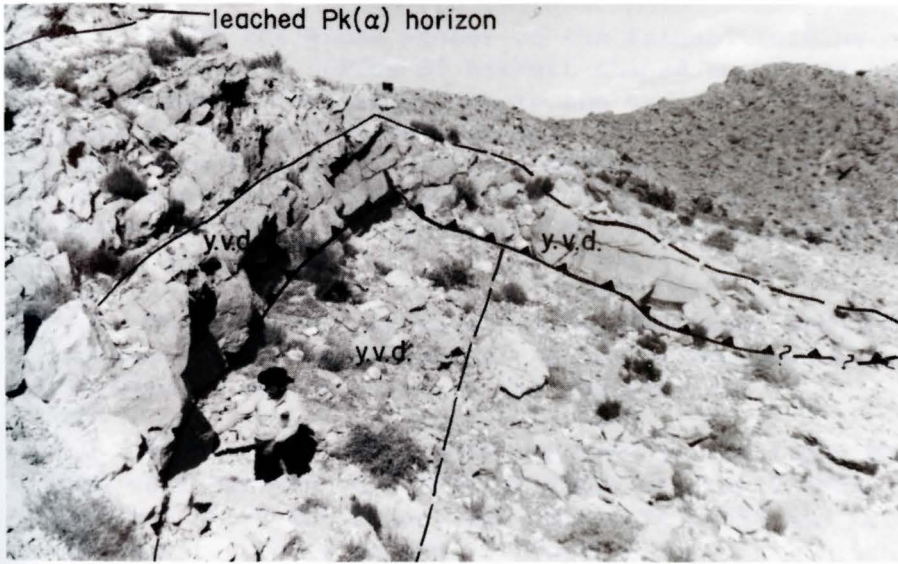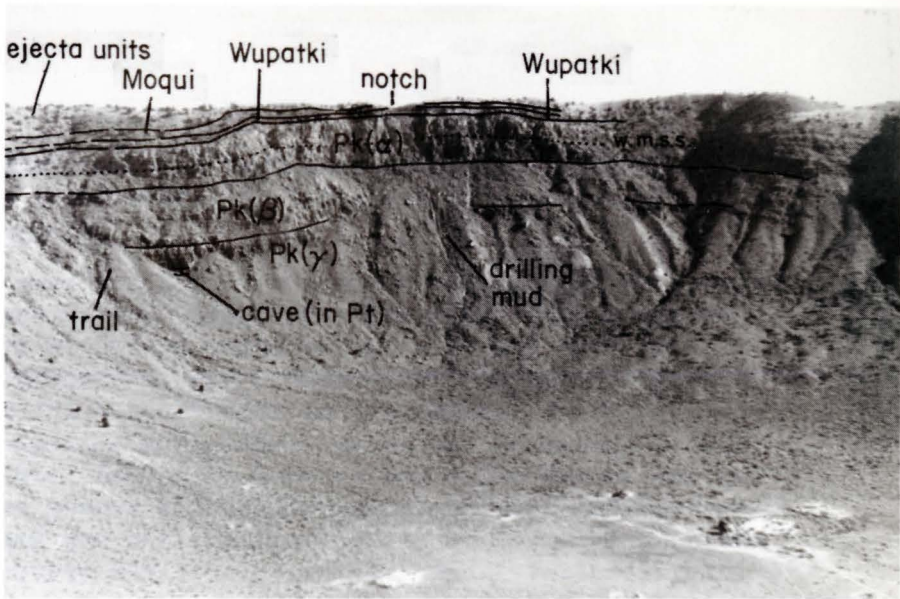w.m.s.s., is shown
with dotted line.

Figure 18a.
Trail Station 2.
View of the upper
thrust fault which
offsets beds in the
upper part of the
Alpha Member of the
Kaibab Formation.
The yellow vuggy
dolomite (y.v.d.)
forms a useful
marker for tracing
faults. Leached
horizon of Alpha
Member (α), is at
upper left.

Figure 18b.
Trail Station 2.
The lower thrust
fault and location
of Trail Station 3

The Beta Member can be distinguished from the underlying Gamma Member and the overlying Alpha Member by its light color and by the lack of well-developed bedding.

The vertical cliff near the top of the south crater wall is formed by the Alpha Member of the Kaibab Formation. The Alpha Member grades upward from medium- to thick-bedded sandy dolomite at the base to medium-bedded dolomite, sandstone, and limestone at the top. Almost exactly in the middle of the Alpha Member is a prominent 2-meter- (7-foot-) thick white sandstone marker bed, which can be traced almost entirely around the crater. Sandstone beds in the Alpha Member are composed of relatively clean quartz sand cemented, in part, by carbonates. Well-developed bedding and the distinctive variety of rock types in the Alpha Member permit detection and tracing of very small faults across the upper part of the bedrock crater rim.

Above the Alpha Member of the Kaibab, forming a rounded pink ledge, or, locally, a series of biscuit-shaped knobs, is the Wupatki Member of the Moenkopi Formation. Where the beds are best exposed, sandstone of the Wupatki is found to be separated from the uppermost beds of the Kaibab by about one foot of fissile red Moenkopi siltstone. About 8 meters (25 feet) of siltstone and fine sandstone of the Moqui Member of the Moenkopi Formation form the lower part of a red slope above the Wupatki sandstone ledge.

The uppermost units on the south crater rim are layers of Moenkopi, Kaibab, and Coconino debris. A nearly continuous layer of Coconino debris is exposed on the crest of the southern rim.

Two thrust faults that cut beds in the Alpha Member of the Kaibab are well exposed just east of trail station 2 (Fig. 18a,b). The two faults are one above the other; the uppermost fault has relatively small displacement. Three meters (10 feet) east of trail station 2, limestone and dolomite beds in the upper part of the Alpha Member are turned up very sharply and locally overturned. The beds here are deformed on the flank of an arch developed over the highest thrust fault. The fault itself is exposed 11 meters (35 feet) to the east of the station. At this exposure, the yellow vuggy dolomite marker bed in the lower plate of the thrust is in contact with the same yellow dolomite bed in the upper plate. About 15 cm (1/2 foot) of yellow dolomite gouge is developed along the fault. Fourteen meters (45 feet) farther to the east, this fault and the yellow vuggy dolomite marker bed in the upper plate bend sharply and trend down the crater wall. The beds in the upper plate are arched over a wedge of Alpha Member rocks about 15 meters (50 feet) across. This wedge has been thrust outward from the center of the crater and under the uppermost bend of the Kaibab. Along the crest of the arch in the upper plate, the beds dip away from the center of the crater about 30 degrees. The fault dips at a steeper angle, probably near 45 degrees. As the repetition in section produced by faulting is about 2 meters (6 feet), the throw on the fault is about 5 meters (15 feet).

Proceed 26 meters (85 feet) in a direction south 55 degrees east, from station 2 to reach trail station 3.

Trail station 3.--At trail station 3 the lower thrust fault displaces the yellow vuggy dolomite marker bed (Fig. 18b). In the lower plate of this lower thrust, the yellow vuggy dolomite extends southeastward from the fault as a prominent yellow ledge that marks a break in slope at the top of the very steep part of the crater wall. Just upslope from the ledge, the fault trends south 70 degrees east, and follows exactly along the Astronaut Trail. Below the trail, the beds strike nearly parallel with the trail and dip away from the center of the crater about 30°. Above the trail, the uppermost beds of the Alpha Member trend directly down the crater wall and terminate abruptly at the fault.

To the west, toward the observation platform, the surface trace of the fault descends diagonally down the crater wall, passing just below a bold outcrop of bedded dolomite. From a gully just to the west, it passes southwestward along the crater wall and passes out of sight around a ridge 35 meters (135 feet) west of trail station 3 (Fig. 19).

To reach trail station 4, the visitor should proceed westward along the trace of the fault, around the corner of the ridge visible from trail station 3, and down a chute to a point directly beneath the observation platform. The trough of this chute follows exactly along the fault. From the base of the chute, walk 8 meters (25 feet) west along a level ledge; then turn around and look back to the east. From the base of the chute, the fault follows the base of the cliff; fault breccia and gouge can be observed at foot level along the inside margin of the ledge.

Trail Station 4.--Looking east, back along the thrust fault from trail station 4, an excellent view is obtained of the white marker sandstone bed in the middle of the Alpha Member of the Kaibab (Fig. 20). The sandstone dips 33 degrees into the crater wall and is truncated by the thrust fault at the base of the chute. The marker sandstone crops out in the upper plate along a nearly vertical cliff. On the cliff it has been stained red by hematitic material washed down from the Moenkopi Formation higher on the crater rim.

Displacement on the fault at this point is such that a dolomite bed about 0.6 meters (2 feet) below the base of the marker sandstone in the upper plate lies directly opposite from the top of the marker sandstone in the lower plate. About 3.3 meters (11 feet) of strata are duplicated by thrust movement. The average dip of the fault here is 47 degrees. Thus, the total throw on the fault is about 13.6 meters (45 feet).

Similar thrust faults are found both high and low along the crater wall on the north and west sides of the crater. They have not been recognized on the south or east sides. Several such thrust faults are present, one above the other, under the structurally high northwest corner of the crater. Directly under the highest point, the Beta Member of the Kaibab is anomalously thick. This anomalous thickness probably is due to repetition of the section

Figure 19.
Trail Station 3, view to west. The surface trace of a thrust fault trends diagonally down along the crater wall. The yellow vuggy dolomite marker bed (y.v.d.) in the upper plate is visible at the upper right, and the white marker sandstone (w.m.s.s.) can be seen in the lower plate in the lower left. To reach Trail Station 4 follow the fault to the point where it disappears behind the ridge below the observation platform.

Figure 20.
Trail Station 4.
View of thrust fault looking east. Displacement of the white marker sandstone (w.m.s.s.) along the fault can be observed easily here. The fault breccia can be traced along the bottom of the cliff.

along a number of thrusts. Several zones of breccia that run sub-parallel with the bedding along the outcrop are present, but, because of the lack of distinctive marker beds in the Beta Member, it is difficult to demonstrate thrust displacement. Probably most of the arching of beds which can be seen in the northwest corner of the crater can be attributed directly to the presence of a stack of underthrust slices.

As thrust faults are only recognized on the north and west sides of the crater and are especially well developed in the northwest corner, it is possible that the distribution of thrust faults provides a clue to the direction of motion of the impacting bolide. The structural evidence suggests that the bolide was traveling from the southeast to the northwest.

From this point the visitor should retrace his steps to trail station 3. The adventurous may wish to follow the marker sandstone around the cliff to the gully below station 3 before climbing up. From station 3 proceed 60 meters (200 feet) east to trail station 5, which is located in the midst of bold red sandstone outcrops of the Wupatki sandstone.

Trail Station 5.--Trail station 5 is by a large outcrop of red sandstone about 6 meters (20 feet) below the top of the Wupatki Member (Fig. 21). The sandstone is crossbedded; the crossbedding is of the festoon, or trough type. Individual crossbed sets are typically about one foot thick. At the top of each crossbed set, the crosslaminae generally are truncated at an angle of about 30 degrees. At the base of these sets, the crosslaminae are truncated at angles generally less than five degrees; in many places the laminae join the base tangentially. This difference in angular relationships of the crosslaminae between the top and base of each set provides an unambiguous method for the determination of top and bottom of beds. Calibrate your eyeball for crossbedding at this outcrop. The method will be put to use in determining the orientation of sandstone blocks in the Moenkopi debris layer upslope and to the right from trail station 5.

Proceed 21 meters (70 feet) to the northeast, angling upslope to a line of red sandstone blocks in the Moenkopi debris layer. At about 11 meters (35 feet), the Astronaut Trail crosses the contact of the Moenkopi debris layer with Moenkopi bedrock. At the top of the Moenkopi debris layer is a line of sandstone blocks (Fig. 22). Each crossbedded block of sandstone can be tested for orientation. The visitor is invited to examine at least half-a-dozen of the large sandstone blocks, or as many as he likes until he is satisfied that all blocks which are still in place in the debris layer are upside down. Follow the Moenkopi debris layer 56 meters (185 feet) to the southeast to trail station 6.

Trail Station 6.--At station 6, with some careful searching, it is possible to identify the exact point on the ground at which the Moenkopi beds turn over and pass into debris. Six meters (20 feet) to the east of this point is a large red sandstone slab (Fig. 23) which has moved slightly downhill from its original position in the debris layer but still preserves its approximate original orientation in the debris. It is easy to establish that this block is still upside down.

41

Figure 21.
Trail Station 5.
Crossbedded sand-
stone of the
Wupatki Member of
the Moenkopi.

Figure 22.
Between Trail Stations 5 and 6.
This line of red sandstone
blocks is in the Moenkopi debris
unit and contains many fragments
which can be shown from the
crossbedding to be inverted.

Figure 23.
Trail Station 6.
Large overturned block
of the Moenkopi debris
unit which has shifted
slightly downhill.

Proceed 66 meters (220 feet) in a direction south 65 degrees east, first following the contour and then dropping very slightly downhill to trail station 7.

Trail Station 7.--At station 7 the contact between the Kaibab debris and the Moenkopi debris is well exposed (Fig. 24). An examination of the blocks at the base of the Kaibab debris layer shows that beds in the upper-most part of the Alpha Member are not represented. Blocks at the base of the Kaibab debris layer at this point are derived from dolomite beds 6 to 9 meters (20 to 30 feet) below the top of the member; rocks from uppermost part of the Kaibab are missing. As the debris layer was peeled out of the crater, it was stretched out to cover a broader area. Because the Kaibab beds deformed by brittle fracture, at the low shock pressures associated with the ejection of the rim debris units, the stretching of the rim debris occurred by spacing out of individual fragments. At any one place in the debris unit, the relative vertical sequence of fragments will be in inverted stratigraphic order, but parts of the stratigraphic section may be expected to be missing.

From station 7 both the Moenkopi debris unit and the underlying Moenkopi bedrock unit drop gradually down the wall of the crater to the southeast. These units can be followed by eye for a distance of 30 to 45 meters (100 to 150 feet). At the approximate position of a shallow gully, both red units are abruptly truncated. Across the gully the beds exposed are in the Alpha Member of the Kaibab Formation. The line at which the red sandstone outcrops are truncated is the surface trace of a large tear fault; the gully is localized along the fault. The fault may be traced down the gully to the southwest to the base of the Kaibab Formation. Rocks on the southeast side of the fault have been raised and displaced outward from the center of the crater farther than the rocks on the northwest side.

The relative displacement on the tear fault, along the gully, is about 24 meters (80 feet). The marker sandstone in the middle of the Alpha Member of the Kaibab on the far side of the fault has been displaced against the Moenkopi debris layer on the near side of the fault (Fig. 25); beds in the upper part of the Beta Member, which form very light-colored outcrops on the far side, are against beds in the upper part of the Alpha Member on the near side of the fault.

About 36 meters (120 feet) from trail station 7, and somewhat lower than the station, the surface trace of the tear fault turns to the left and passes at an angle across the crater wall about 15 meters (50 feet) upslope from station 7. It can be followed another 45 meters (150 feet) in a north-west direction. A large slab of relatively massive dolomite above station 7, which dips about 55 degrees towards the observer, is part of a flap of overturned bedrock suspended in the debris unit. The tear fault passes just below this slab.

As in the case of many other tear faults in the crater wall, the trend of the large tear fault near trail station 7 is controlled by pre-existing joints. Two prominent sets of joints cut the Kaibab and Moenkopi Formations in the vicinity of the crater and in nearby parts of the Colorado Plateau

Figure 24.
Trail Station 7.
At the contact be-
tween Kaibab debris,
Qk, and Moenkopi
debris, Qm.

Figure 25.
Trail Station 7.
View to east of
of tear fault.
Beds in Alpha
Member of Kaibab,
Pk(α), on far side
of fault are
against Kaibab
debris, Qk, and
Moenkopi debris,
Qm, on near side.
The white marker
sandstone,
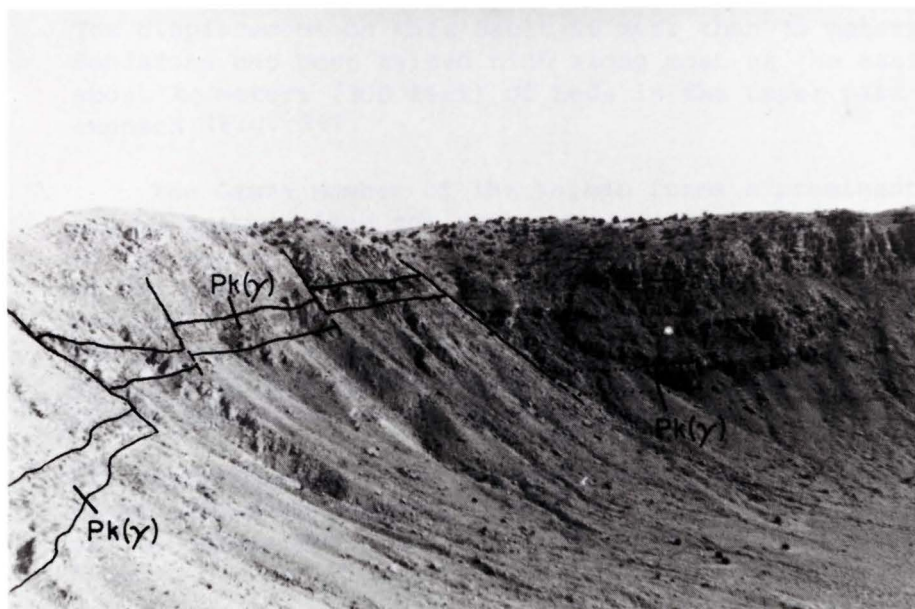w.m.s.s., and Beta
Member, Pk(β),
are raised high
on crater wall.

Figure 26.
Trail Station 7,
view toward south-
east corner of
crater. Several
tear faults displace
the Gamma Member
of the Kaibab
Formation, Pk(γ).

Both joint sets are vertical or nearly vertical, where the bedding is flat or very gently dipping; they strike at nearly right angles to one another. One joint set trends approximately northwest, and the other joint set trends northeast. The lower part of the tear fault near station 7 has been controlled by a northeast-trending joint; the upper part of the fault was controlled by a northwest-trending joint.

As beds were peeled back along the crater wall, during the formation of the crater, rocks on the east side of the tear fault were lifted high on the crater wall and rotated, in places, more than 90 degrees. The fault surface itself, where it bounds the lower edge of the suspended flap, has been rotated about 125 degrees around an axis approximately parallel with the original strike of the fault. In order to visualize the original position of the beds now in the suspended flap, face the center of the crater, while standing or sitting at station 7, and put your hands back over your head tilted backward at about 35 degrees from the vertical. Now rotate your hands and arms forward until they are level, and imagine that you have rotated the flap back to a position in front of you and at the level of the upper part of the Kaibab Formation; the beds in the flap would lie a little closer to the center of the crater than the present crater wall.

Large tear faults occur in all four corners of the crater, and these tear faults have controlled the shape of the crater rim. As seen from the air, Meteor Crater is approximately square in outline. The tear faults occur along the diagonals of the square. These diagonals are controlled, in turn, by the regional joint sets, the northwest-trending diagonal by the northwest striking joint set, and the northeast-trending diagonal by the northeast joint set.

Large displacement has occurred along the tear fault in the southeast corner of the crater. Beds in the upper part of the Coconino Sandstone, along the east wall of the crater, have been displaced against beds in the upper part of the Beta Member of the Kaibab on the south wall of the crater. The displacement on this fault is more than 45 meters (150 feet). Coconino Sandstone has been raised high along most of the east wall of the crater; about 90 meters (300 feet) of beds in the upper part of the Coconino are exposed (Fig. 26).

The Gamma Member of the Kaibab forms a prominent yellow cliff which can be traced along the east crater wall. Near the southeast corner of the crater this cliff occurs about 3/4 of the distance from the floor of the crater to the rim. It drops gradually in elevation to the north. The cliff is offset at several places by minor tear faults in the east wall. The most prominent of these tear faults is about midway between the southeast corner and the northeast corner of the crater, and offsets the base of the Kaibab Formation by about 100 feet.

From station 7 the Astronaut Trail gradually ascends the crater wall in an east-southeasterly direction, heading for the prominent high point on the crater rim. At 20 meters (65 feet) the trail crosses the tear faults. Station 8 lies 105 meters (350 feet) from station 7.

45

Trail Station 8.--Station 8 is at the contact of Kaibab debris and Kaibab bedrock. Blocks in the Kaibab debris, near the contact, generally dip away from the center of the crater. Most of them have been rotated through more than 200 degrees. They are derived from the upper part of the Alpha Member of the Kaibab. Bedrock at the contact is overturned and dips about 60 degrees towards the center of the crater. Downslope, the dip steepens, passes through the vertical, and then rapidly becomes more gentle.

Neither Moenkopi bedrock nor Moenkopi debris is exposed at this place on the crater rim. To reach these units from station 8, it would be necessary to drive an inclined shaft. With a shaft inclined away from the center of the crater at a vertical angle of about 45 degrees, Moenkopi rocks would be encountered at a depth of about 4-1/2 to 6 meters (15 to 20 feet).

Looking back to the northwest along the crater wall from station 8, it is relatively easy to pick out the boundaries of the bedrock flap suspended in debris above station 7 (Fig. 27). Rocks in the bedrock flap form bold outcrops with well-developed bedding, which dips approximately parallel with the slope of the crater wall. These beds are overturned. The Kaibab debris unit surrounding the bedrock flap weathers to a smoother surface than the bedrock. It is difficult to trace by eye the contact of the Kaibab debris with bedrock towards station 8; at station 8, blocks in the debris are coarser grained than they are directly above the bedrock flap.

Proceed 36 meters (120 feet) southeast from trail station 8. Trail station 9 is by the first bold outcrop of buff-colored sandstone in the Wupatki Member of the Moenkopi. The Astronaut Trail crosses the contact between the Kaibab and Moenkopi at 24 meters (80 feet).

Trail Station 9.--Looking back to the northwest from station 9, the Moenkopi bedrock and debris can be seen underlying overturned beds and debris of the Alpha Member of the Kaibab (Fig. 28). Moenkopi bedrock and debris units here form the core of an overturned syncline. They are enclosed in folded Kaibab somewhat like a hot dog in a hot dog bun. In the upper limb of the syncline, the stratigraphically highest beds of the Kaibab pass outward gradationally into debris.

Proceed 44 meters (180 feet) south-southeast of station 9 to trail station 10. The Astronaut Trail follows the outcrop of sandstone of the Wupatki Member of the Moenkopi. Outcrops of the leached uppermost unit of the Kaibab Formation can be seen downslope just below the trail.

Trail Station 10.--Station 10 is at the contact of the Moenkopi Formation and the Kaibab Formation. Looking to the southeast from station 10, outcrops of Moenkopi bedrock and Moenkopi debris can be seen sandwiched between bedrock Kaibab below and the layer of Kaibab debris above, which forms the crest of the crater rim (Fig. 29). Large blocks in the Kaibab debris along the rim crest are derived from beds in the Alpha Member, which can be seen cropping out on the slope below. Dips in the Alpha Member are about 45 degrees away from the center of the crater.

Figure 27.
Trail Station 8.
View to northwest.
A large flap of
Kaibab bedrock,
Pk(α), is suspended
in Kaibab debris,
Qk.

Qk

Qk

Pk(α)

Figure 28.
Trail Station 9.
Moenkopi bedrock and
debris, Ŧm, under
lie overturned
Kaibab bedrock and
debris, Pk, in the
core of an over-
turned syncline.

Pk

Ŧm

East and West Sunset Buttes
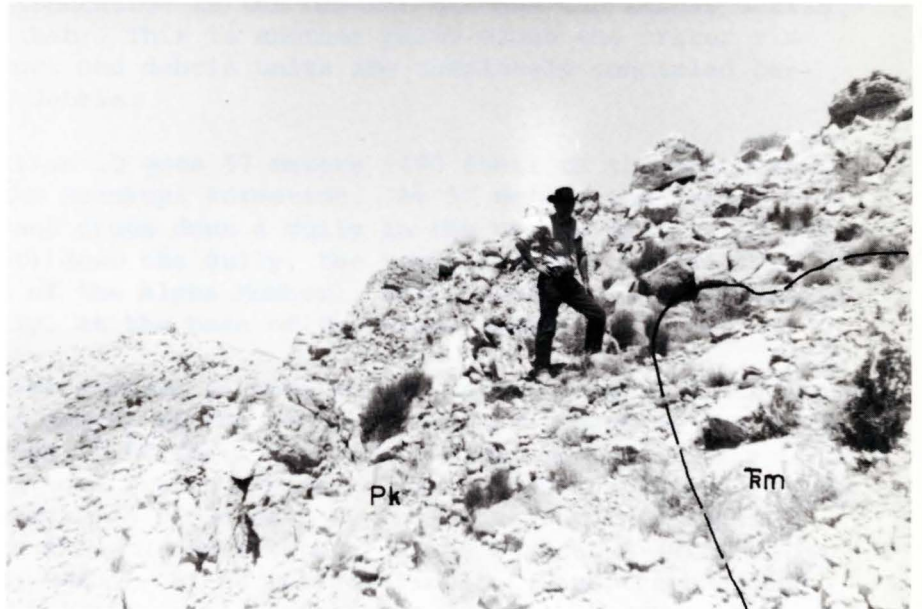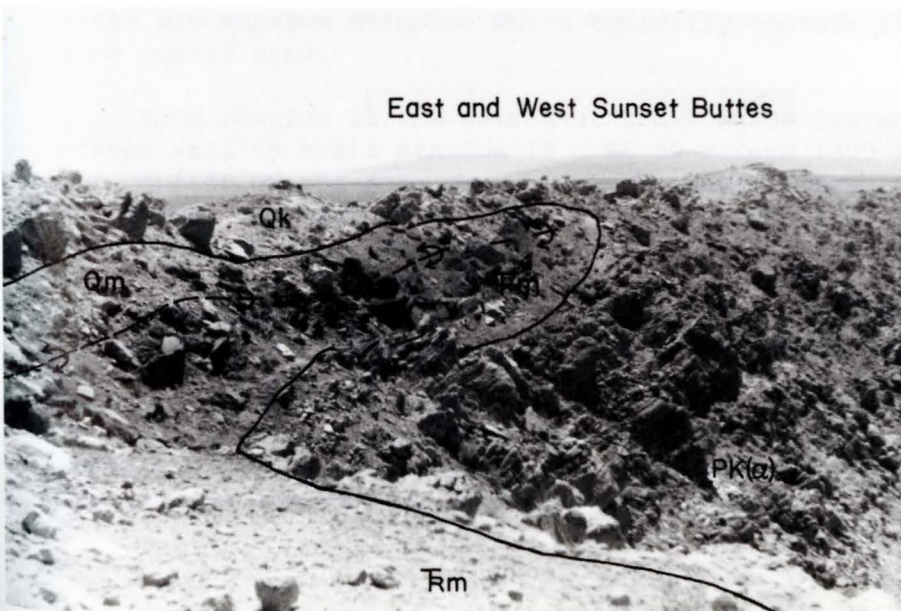
Qk

Qm

Ŧm

Pk(α)

Figure 29.
Trail Station 10.
View to southeast.
Moenkopi Sandstone,
Ŧm, and Moenkopi
debris units, Qm,
form the core of an
overturned syncline.
Kaibab debris, Qk,
forms the crest of
the rim. The Alpha
Member of the
Kaibab, Pk(α),
forms the slope
below.

About 150 meters (500 feet) to the south-southeast along the crater rim, uppermost beds of the Kaibab are peeled back sharply and can be traced up the wall to the rim crest where they pass into Kaibab debris. Here the Moenkopi bedrock and debris units again form the core of an overturned syncline, as near station 9. The contact of the Moenkopi debris unit on the bedrock Moenkopi, at the axial plane of the fold, was essentially the original ground surface at the time the crater was formed. Where the Moenkopi bedrock unit is peeled up and passes into Moenkopi debris in the core of the syncline, this contact terminates abruptly at the hinge line of the fold.

Looking to the south under the highest point on the southern crater rim, under a triangulation marker, beds of the Alpha Member of the Kaibab can be seen which turn up vertically. Near the rim crest these upturned beds appear to be truncated abruptly and overlain by nearly structureless material. The line of truncation is the contact between the Kaibab debris unit and the bedrock Kaibab. This is another place along the crater rim where the Moenkopi bedrock and debris units are completely concealed beneath overturned Kaibab debris.

The trail from station 10 goes 57 meters (190 feet) to the southeast, following the base of the Moenkopi Formation. At 57 meters the trail turns to the southwest and drops down a gully in the crater wall (Fig. 30). Eighteen meters (90 feet) down the gully, the trail crosses the marker sandstone in the middle of the Alpha Member. Trail station 11 is 50 meters (190 feet) down the gully, at the base of the Alpha Member.

Trail Station 11.--At station 11,beds in the Kaibab Formation dip about 40 degrees away from the center of the crater. The basal beds of the Alpha Member crop out as a steep cliff that, in places, forms an overhanging ledge. (Fig. 31). They weather to a light grayish-yellow. Beds in the underlying Beta Member form a more uniform slope with few bold outcropping ledges. They are a pale greenish-gray to nearly white on the weathered surface. In contrast to the Alpha Member, it is very difficult to observe bedding in the Beta Member in the outcrops along the crater wall. The Beta Member rocks are massive dolomite which typically contain about 20 percent very fine quartz sand.

From station 11 the Astronaut Trail winds 120 meters (400 feet) down the crater wall to trail station 12. At 90 meters (300 feet) the trail crosses the contact of the Beta Member and the Gamma Member of the Kaibab. Station 12 is near the apex of a large talus cone, below a prominent spire of rock formed by the lower part of the Beta Member of the Kaibab.

Trail Station 12.--Looking to the south from station 12 along the crater wall, the Gamma Member of the Kaibab forms a prominent yellowish-brown cliff (Fig. 32). At the base of this cliff, white sandstone is interbedded with the yellowish sandy dolomite. Two and six-tenths meters (9 feet) of interbedded sandstone and sandy dolomite are present, which constitute the Toroweap Formation. In most places, the base of the Toroweap is precisely at the base of the cliff.
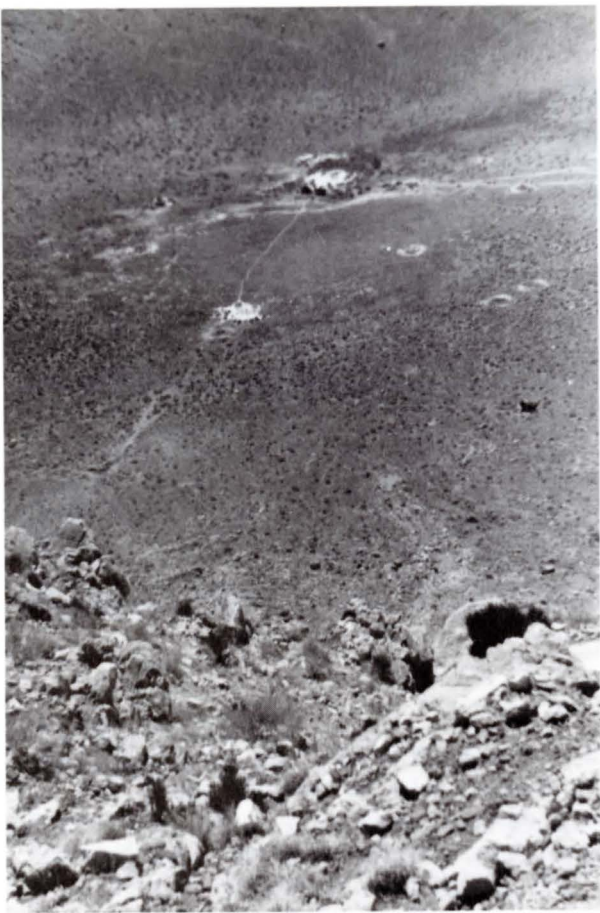
Figure 30.
View of top of gully 57 meters
(190 feet) southeast of Trail
Station 10. The trail drops
down the gully.

Figure 31.
Trail Station 11.
View to south.
Beds of the Alpha
Member of the Kaibab,
Pk(α), dip about 40°
away from the center
of the crater. The
massive Beta Member,
Pk(β) is exposed
on the slope
below.

49

Figure 32 (above).
Trail Station 12. View to south. Cliff of the Gamma Member of the Kaibab Formation, Pk(γ), is overlain by slope-forming Beta Member, Pk(β), and underlain by the Toroweap Formation, Pt, and the Coconino Sandstone, Pc.

Figure 33 (right).
Chute eroded into a breccia zone 12 meters (40 feet) north of Trail Station 14. Faint bedding planes can be traced through the breccia.

Figure 34.
Small outcrop of mixed debris between Trail Station 12 and the mouth of the chute. Pieces of rock from all formations are intermixed in this deposit. PLEASE do not damage or remove samples from this small outcrop.

Below the Toroweap are rounded to subdued outcrops of fractured, light gray to white sandstone. This sandstone is the upper part of the Coconino Sandstone. As much as 30 meters (100 feet) of the uppermost Coconino Sandstone beds are locally exposed in gullies and in subdued ridges between the more prominent talus cones.

Twelve meters (40 feet) north of station 12 is the mouth of an unusual chute in the wall of the crater (Fig. 33). This chute has been eroded in a northwest-trending zone of breccia, which follows a prominent northwest-trending joint. The breccia is developed in Gamma and Beta Members of the Kaibab. Faint bedding planes marked by light greenish-gray clayey bands in the Kaibab dolomite, which can be traced through the breccia, show that, although the rocks have been shattered, there has been no shear or fault displacement in the breccia.

Between station 12 and the mouth of the chute is a small outcrop of mixed debris, which lies beneath eroded talus (Fig. 34). Pieces of rock from all formations exposed in the crater wall are represented in this debris. Some of these pieces are relatively strongly shocked. This mixed debris is an outcrop of a layer of fallout material, preserved beneath younger sedimentary deposits, which lines the lower crater wall and the crater floor. A more extensive outcrop of mixed debris will be seen at trail station 13.

From station 12 to station 13 the Astronaut Trail drops down along the edge of the talus cone to the south and then follows along the base of the Coconino Sandstone outcrop. At 60 meters (200 feet), giant cross-bedding in the Coconino Sandstone is especially well exposed (Fig. 35). Large crossbed sets seen here may be thought of as fossil sand dunes. The Coconino Sandstone consists chiefly of windblown sand. In places, medium-grained quartz constitutes more than 99 percent of the rock. Station 13 is about 90 meters (300 feet) south of station 12, at the contact of talus against Coconino Sandstone.

Trail Station 13.--Beneath the talus at station 13 is a good exposure of the mixed debris or fallout unit which lined the original crater (Fig. 36). Here the fallout unit rests upon Coconino Sandstone in the bedrock crater wall. The contact between the fallout and the bedrock dips towards the crater at an angle of nearly 80 degrees. The fallout is overlain by Pleistocene talus, which is composed chiefly of relatively coarse blocks derived from higher parts of the crater wall.

All formations intersected by the crater are represented in the fallout unit. The bulk of the fallout is composed of pieces derived from the Kaibab Formation, which are light gray in color. It is flected by easily recognized red fragments of Moenkopi. Close examination of the exposure reveals that there are also many pieces of relatively unshocked Coconino Sandstone.

Rare fragments of strongly shocked rock are scattered through the mixed debris. These include fragments of Coconino, showing all five stages of shock metamorphosism, and also lapilli of shock melted Kaibab dolomite. When this outcrop was first visited by Shoemaker in 1957, two oxidized fragments of iron meteorite embedded in the mixed debris were exposed. In subsequent

Figure 35. 60 meters (200 feet) south of Trail
Station 12. Giant crossbedding in the Coconino
Sandstone.

Figure 36. Trail Station 13. Beneath the
Pleistocene talus, Qpt, is an outcrop of the
mixed debris unit, Qd, which rests directly on
Coconino Sandstone, Pc, in the bedrock wall of
the crater.

years these two objects were washed down the slope; they now reside in the collection of the U.S. Geological Survey. Other oxidized fragments of meteorite have been found in exposures of the fallout layer on the north and west walls of the crater. The visitor is requested not to deface this exposure in any way, as it is one of the most representative exposures of the fallout unit in the crater.

Station 13 is located just below a line along the crater wall which divides the wall into two easily recognized parts: 1) an upper part which has been eroded back since the crater was formed, and 2) a lower part which has been covered by detritus derived from erosion of the upper part. All of the natural exposures of the fallout layer occurr just below this line, in gullies where the oldest Pleistocene talus has been partly stripped away.

Proceed 240 meters (800 feet) down the crater wall to station 14. Walk in the direction of the nearest shaft on the margin of the playa beds. The shaft can be recognized by a mound of light-colored material which has been dumped around it. Station 14 is about 23 meters (75 feet) beyond the burned-out remains of an old drilling rig on the crater floor.

Trail Station 14.--Looking back at the crater wall from station 14, two different units can be readily distinguished in the talus and alluvial fill of the crater (Fig. 37). The oldest unit is represented by triangular patches of talus, which form a series of fingers reaching up the crater wall. On the basis of correlation of soil profiles in the talus with soil profiles of the Hopi Buttes region, this talus can be shown to be equivalent to parts of the Jeddito Formation of Pleistocene age in the Hopi Buttes. The talus is of late Pleistocene age, but it is not the latest Pleistocene deposit in the crater. This talus probably was laid down during a pluvial episode in southwestern United States corresponding to one of the mid-Wisconsin glacial advances in the central United States. A period of slope stability and soil formation followed the deposition of the oldest talus. It was then deeply cut by gullies which dissect the talus into the triangular patches we see today.

Very coarse alluvial fans extending out onto the crater floor head in gullies that cut through the oldest talus. Most of the alluvial fans have a soil developed on them which corresponds to the highest soil in the Jeddito Formation. These fans are late Pleistocene age, and the gullying associated with them is, therefore, also Pleistocene. Probably the fans were developed in a pluvial episode in the southwest corresponding to the last advance of the Wisconsin continental ice. Levied channels pre-served on parts of these fans attest to the small degree of erosion that has occurred since the end of the Pleistocene.

The alluvial fans have been eroded, however, along their lower margins. Locally, in a zone surrounding the present playa, as much as five feet of Pleistocene alluvium has been eroded. Station 14 is located at the upper edge of the erosional surface developed during this post-Pleistocene dis-section. A very thin veneer of relatively fine-grained Holocene alluvium extends up from the edge of the playa along shallow gullies cutting into the Pleistocene alluvium.
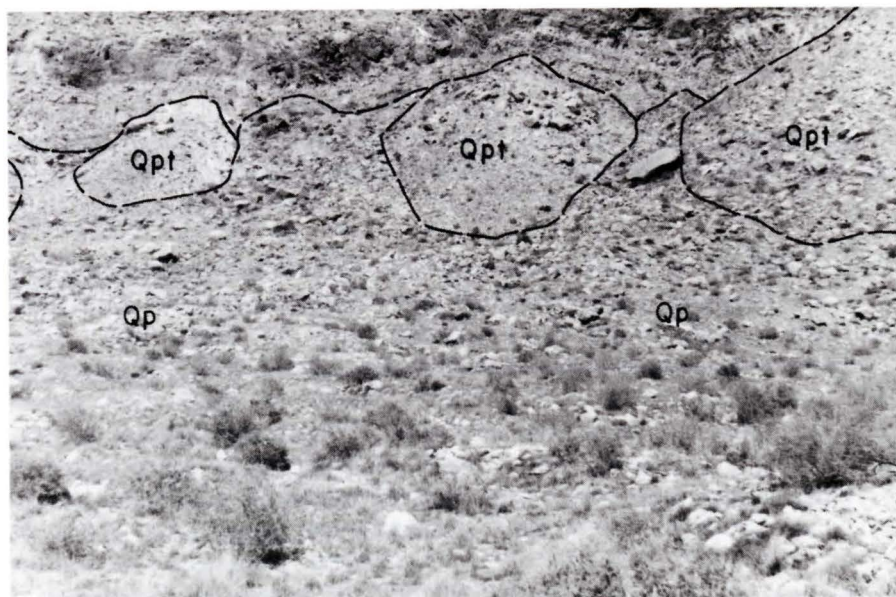
Figure 37. Trail Station 14.
View to east showing Pleistocene talus, Qpt, and
younger Pleistocene alluvium, Qp, on the lower
wall of the crater.

Figure 38. Trail Station 15.
Dump from shaft II contains material from the
fallout unit, the allogenic breccia and the
Pleistocene lake beds that underlie the crater
floor.

Proceed to station 15, which is 105 meters (350 feet) west of station 14, on the dump on the east side of shaft II near the east margin of the playa.

Trail Station 15.--The dump on the east side of shaft II (Fig. 38) contains material excavated from the fallout unit exposed in a lower part of the shaft. The shaft is 43.3 meters (145 feet) deep. The upper 30 meters (100 feet) of the shaft penetrated lake beds. Below the lake beds is 10.3 meters (35 feet) of mixed debris of the fallout unit. Here the fallout unit is almost perfectly massive but shows a very slight grading in average grain size from base to top. The lowest 1.3 meters (5 feet) of the fallout unit are distinctly coarser than the upper part. Below the fallout unit, the shaft penetrated 3 meters (10 feet) into the allogenic breccia lens that underlies the crater. Here the allogenic breccia is composed entirely of fragments of Coconino Sandstone, ranging in size from microscopic splinters up to blocks more than a meter across. The pieces of sandstone in the breccia exhibit a wide range of shock metamorphism. The presence of fragments showing widely different degrees of shock metamorphism in close juxtaposition shows that the breccia has been stirred or mixed.

The dump of a shaft, like throwout from an impact crater, tends to have inverted stratigraphy. The deepest material excavated from the shaft is the last to be placed on the dump. As this shaft was dug, however, the miners tended to dump material from different depths on different sides of the shaft. Thus, the surface of the dump on the east side of the shaft is material excavated from the fallout unit; on the southwest side of the dump, the surface material is from the allogenic breccia at the base of the shaft; on the northwest side of the dump, material excavated from the lake beds is exposed. The lake bed material is dominantly very thinly laminated, calcareous siltstone. Abundant fresh-water fossils can be found in some pieces.

The part of the dump derived from the fallout unit is an especially good collecting ground for shocked Coconino Sandstone. Many pieces studied by Kieffer were collected from this locality. Examination of the base of the lake beds in the shaft shows that they rest directly on the fallout unit. There are no intervening alluvial deposits. Thus, it is clear that a lake formed in the crater immediately after it was opened up. The groundwater table must have been higher than the floor of the initial crater, i.e., less than 30 meters (100 feet) below the present playa surface. At the present time the groundwater table is 65 meters (210 feet) below the playa surface. The conclusion that the water table was more than 30 meters (100 feet) higher than it is at present, at the time the crater was formed, is consistent with the late Pleistocene age inferred from soil profiles on the oldest talus exposed on the crater walls. Apparently the crater was formed during a period when the rainfall and recharge of groundwater was greater than at present, during a pluvial episode in the southwest.

The lower five feet of lake beds in the shaft contain many blocks of pumiceous lechatelierite. Some of these pieces are more than 30 cm across.

Their stratigraphic distribution indicates that these very low density objects floated for a time in the lake, as the water rose above the crater floor. Placed in a jar of water, pieces on the order of 5 to 8 cm (2 to 3 inches) across will float for several weeks before becoming too water-logged to remain bouyant. Most of the frothy pieces of lechatelierite probably were derived directly from the fallout on the floor. Some, however, may have been washed in from nearby parts of the crater walls.

Proceed 81 meters (280 feet) east from station 15 to station 16, by a shallow pit dug in the playa beds. Along the trail, small hollows between clumps of grass on the playa beds are partially covered with fine black particles. These particles are basaltic ash from Sunset Crater, which is being continually redistributed on the crater floor by the wind.

Trail Station 16.--A careful examination of the playa beds on the edge of the pit at station 16 reveals two layers rich in Sunset Crater ash about 0.3 m (1 foot) beneath the original surface (Fig. 39). The lowest level of the ash marks the position of the playa floor at the time of eruption of Sunset Crater. In the last 900 years, about 0.3 m (1 foot) of playa beds have been deposited in the crater floor. The total thickness of these playa beds, where exposed in the wall of the main shaft, is 1.8 meters (6 feet). The playa beds are composed chiefly of pink aeolian silt blown in from outside the crater. These pink silt beds represent the Holocene record of deposition in the center of the crater. They rest unconformably on frost-heaved Pleistocene lake beds at the collar of the main shaft.

From the pit at station 16, the Astronaut Trail heads 120 meters (400 feet) west-northwest to a broad 6-meter- (20-foot-) high ridge in the floor of the crater referred to by D. M. Barringer as "Silica Hill." Station 17 is located at an exposure of Pleistocene lake sediments about 21 meters (70 feet) southwest of shaft VI, near the summit of "Silica Hill."

On the way to "Silica Hill," the visitor may wish to make a detour to inspect the remains of an old steam boiler and winch, just east of the Main Shaft in the crater floor (Fig. 40). This equipment was used to operate the hoist of the Main Shaft. The boiler and winch were assembled from parts transported to the floor of the crater on mule back.

The Main Shaft, originally 69 meters (230 feet) deep, is located very close to the center of the crater. It was a two-compartment shaft designed by Barringer for commercial production of meteoritic iron ore, which he expected to find in large quantity under the crater. At a depth of 63 meters (210 feet), the shaft reached the water table. An heroic effort to pump out the water succeeded in drawing down the local water level about 6 meters (20 feet), and the shaft was deepened by this amount. Then the walls of the shaft collapsed near the bottom, and it was abandoned.

Figure 39.
Trail Station 16.
A layer rich in ash
from Sunset Crater
can be found in the
playa beds exposed
in this pit about
0.3 meters beneath
the surface.

Figure 40.
Remains of steam
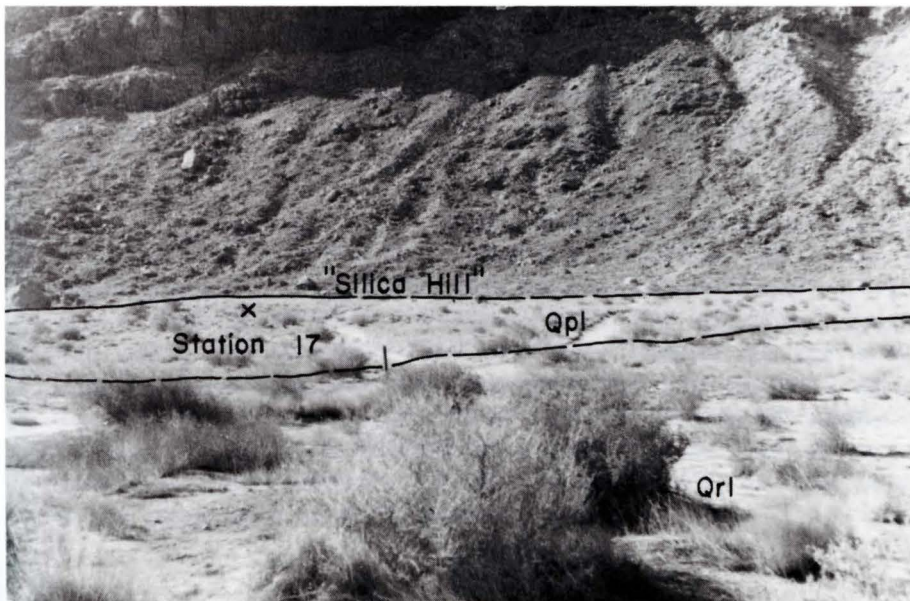boiler and winch
used to operate
hoist in Main
Shaft.

Figure 41.
View to northeast
toward station 17
in Pleistocene
lake beds, Qpl, on
"Silica Hill."
Playa beds, Qrl,
are in foreground.

Trail Station 17.--"Silica Hill" (Fig. 41) is underlain entirely by Pleistocene lake beds. The presence of the lake beds at the summit of the hill shows that, at one time, the lake stood at least 6 meters (20 feet) above the present playa. The highest lake beds are 69 meters (230 feet) above the present water table. At sometime in the late-Pleistocene the water table was at least this high or higher.

Six shafts in the crater floor partly surround "Silica Hill"; four of these, shafts I, II, IV, and V, were investigated and sampled by Shoemaker in 1957. Subsequently, all but two of the shafts have been filled in by Meteor Crater Enterprises to eliminate hazards to visitors. In each shaft examined, a series of three basaltic ash beds was found in the upper Pleistocene lake beds about 5 meters (15 to 18 feet) beneath the surface. this ash was deposited during the eruption of a late Pleistocene volcano near the eastern end of the San Francisco volcanic field, possibly Merriam Crater.

No basaltic ash beds were found in shaft IV in the summit of "Silica Hill." Ten and a half meters (35 feet) of lake beds were exposed in this shaft, and the highest beds contain abundant dessication breccias. It appears likely that "Silica Hill" was above lake level at the time that the three basaltic ash beds were laid down around it. Evidently, the lake beds exposed in shaft VI represent the middle or lower part of the lake bed sequence. If this is true, the base of the lake beds under the hill is at least 15 meters (50 feet) higher than the base of the lake beds under the playa. Thus, the hill appears to be located over a small, somewhat off-center, central peak on the original crater floor.

In shaft I, near the foot of the crater wall, Pleistocene alluvium is interbedded with Pleistocene lake deposits. Probably the Pleistocene lake beds interfinger with Pleistocene alluvium in a ring around the foot of the crater wall. The latest Pleistocene alluvium has covered over the highest lake beds in this ring.

Proceed 300 meters (1000 feet) in a direction slightly east of north. The Astronaut Trail lies east of the main trail on the north crater wall. It enters a gully just above a dump from an old excavation near the foot of the crater wall. Station 18 is in the gully, about 45 meters (150 feet) north of the dump.

Trail Station 18.--Three different geologic units are exposed in the west wall of the gully at station 18 (Fig. 42). The lowest unit is allogenic breccia which, at this place, is composed entirely of fragments of the Kaibab Formation. Fragments in the breccia along the west wall of the gully are derived from the Beta Member of the Kaibab; their mean size here is much smaller than average for the breccia as a whole. On up the gully, on the east side, very coarse blocks of sandy dolomite are present in the breccia. A prominent yellow block just above station 18 is derived from the Gamma Member; other coarse blocks in the breccia are from the basal part of the Beta Member.
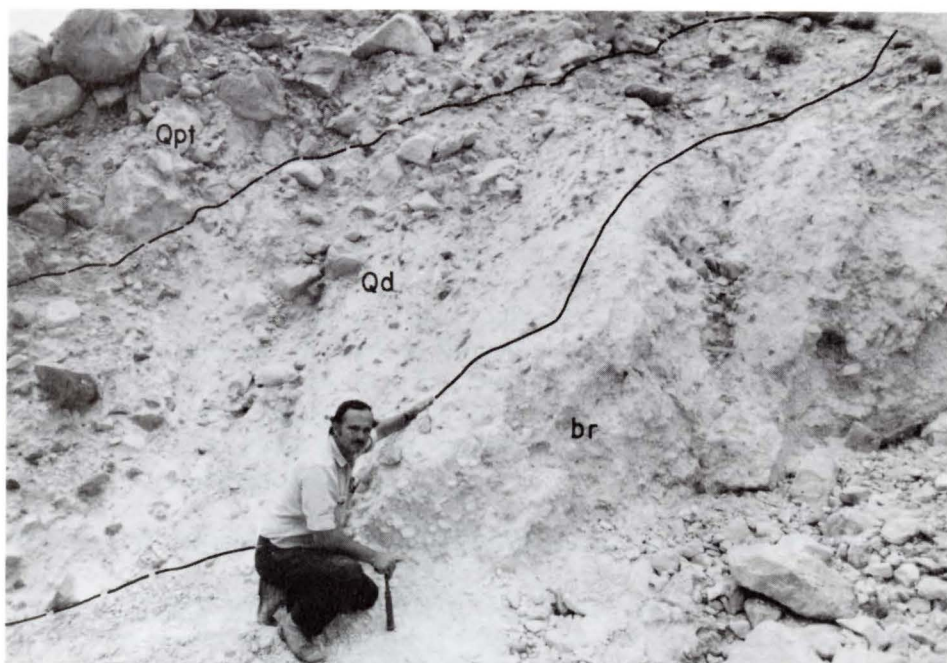
Figure 42. Trail Station 18. View looking west at
exposure of allogenic breccia, br, fallout unit, Qd, and
Pleistocene talus, Qpt, in gully on north wall of crater.
Dark fragments in fallout unit are pieces of Moenkopi
sandstone and siltstone.

Figure 43. Trail Station 19. Exposure of Coconino
Sandstone, Pc, near head of gully on north wall of crater.
Allogenic breccia, br, resting on the Coconino Sandstone
has been displaced more than 30 meters (100 feet) down
the crater wall.

Above the breccia, a lens of fallout material, up to 1.5 meters (5 feet) thick, rests in a local depression in the top of the breccia. Red pieces of Moenkopi sandstone and siltstone and brilliant white fragments of shocked Coconino Sandstone can be recognized in the fallout.

Pleistocene talus rests unconformably on the local lens of fallout material and elsewhere on the allogenic breccia along the west wall of the gully. In most places the fallout layer has been stripped away prior to deposition of the talus, but a few thin remnants of fallout material can be found at the base of the talus farther up the gully, in addition to the lens at station 18.

Proceed 45 meters (150 feet north) along gully to station 19.

Trail Station 19.--At station 19, bedrock Coconino Sandstone is exposed on the east wall of the gully. It is overlain, at this point, by allogenic breccia composed of fragments of the Beta Member of the Kaibab (Fig. 43). About 12 meters (40 feet) farther up the crater wall, the gully heads against a cliff formed by the Gamma Member of the Kaibab and the Toroweap Formation. Higher up along the crater wall, craggy outcrops of the Beta Member form part of the skyline.

The breccia at this station has been displaced down the crater wall more than 30 meters (100 feet). Similar downward and inward displacement of the upper edges of the lens of allogenic breccia can be documented on all four sides of the crater. The centripetal movement of the breccia probably is responsible for the development of the central peak thought to underlie the lake beds at "Silica Hill." A peak should have formed near the point of convergence of flow. The occurrence of fallout in contact with bedrock on the east wall of the crater, seen at station 13, suggests that flow of the breccia and the presumed concomitant development of a central peak took place before deposition of the fallout.

From station 19 the trail goes diagonally up the crater wall to the northeast. Station 20 is about 30 meters (100 feet) from station 19.

Trail Station 20.--East of station 20 the lowermost beds of the Gamma Member of the Kaibab and upper beds of the Toroweap Formation are duplicated by thrust faulting (Fig. 44). Two bold outcrops of the Gamma Member in contact with the Toroweap may be seen in the gully immediately to the east of the station. Below the lowermost of these outcrops is an extensive exposure of the Coconino Sandstone. The thrust fault is exposed at the foot of the upper outcrop. This fault can be traced eastward 60 meters (200 feet) along the crater wall. It passes just above a small juniper tree, beyond the second gully to the east. The Toroweap-Kaibab contact in the upper plate is exposed about 3 meters (10 feet) upslope from the tree. The same contact can also be found in the lower plate about 12 meters (40 feet) downslope from the tree. Along this sector of the crater wall, thrust faults cut beds near the lowest bedrock outcrops and also near the highest outcrops.

Figure 44. Trail Station 20. View to east from station 20 showing thrust fault and repeated section of Toroweap Formation, Pt, and the Gamma Member of the Kaibab, Pk(γ).

Figure 45. Trail Station 21. Authigenic breccia exposed along crater wall east of station 21.

Proceed 90 meters (300 feet) east-northeast along the crater wall to station 21. Station 21 is below and slightly west of the observation platform.

Trail Station 21.--A broad band of authigenic breccia is exposed along the crater wall east of station 21 (Fig. 45). This band is developed primarily in the lower part of the Beta Member of the Kaibab. Because the Beta Member is so massive, it is nearly impossible to demonstrate whether there has been any displacement of beds in the breccia. Distinct zones of crushing, which dip $40°$ to $60°$ outward from the center of the crater, can be seen in the breccia. In places, dolomite of the Beta Member has been very finely pulverized in these zones. Large blocks of relatively uncrushed dolomite are preserved locally between the crush zones. Elsewhere, the fragments in the breccia exhibit a size distribution somewhat similar to that seen in the rim debris units. As the overall apparent thickness of the Beta Member along this part of the Crater wall is greater than normal, it is likely that the breccia represents a broad zone of distributive shear, along which the bedrock lower in the crater wall has been thrust beneath the bedrock higher in the wall.

From this point the Astronaut Trail leads directly up the crater wall and joins the main crater rim trail just west of the observation platform.
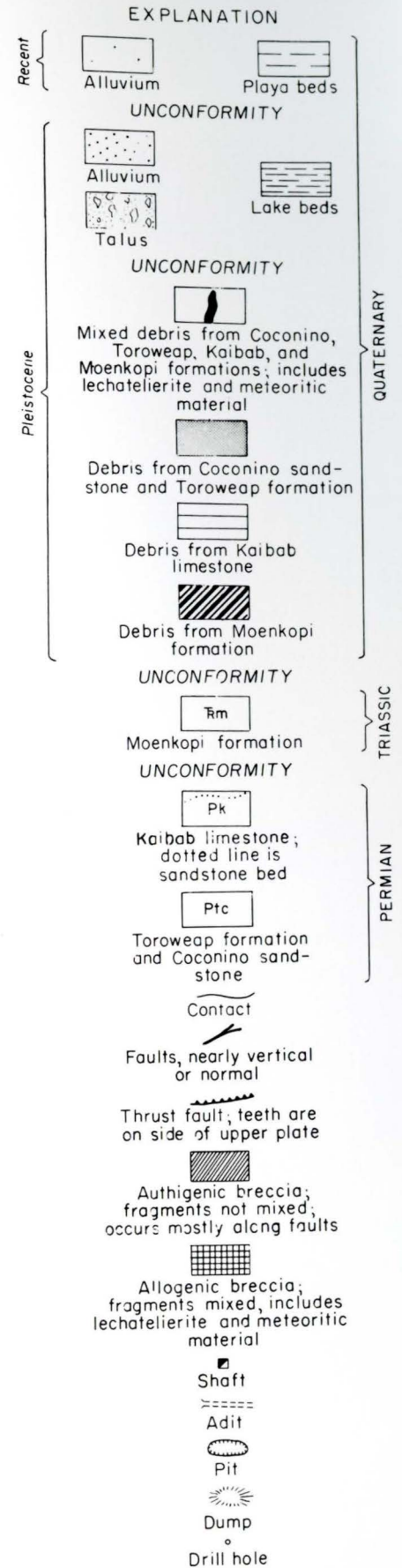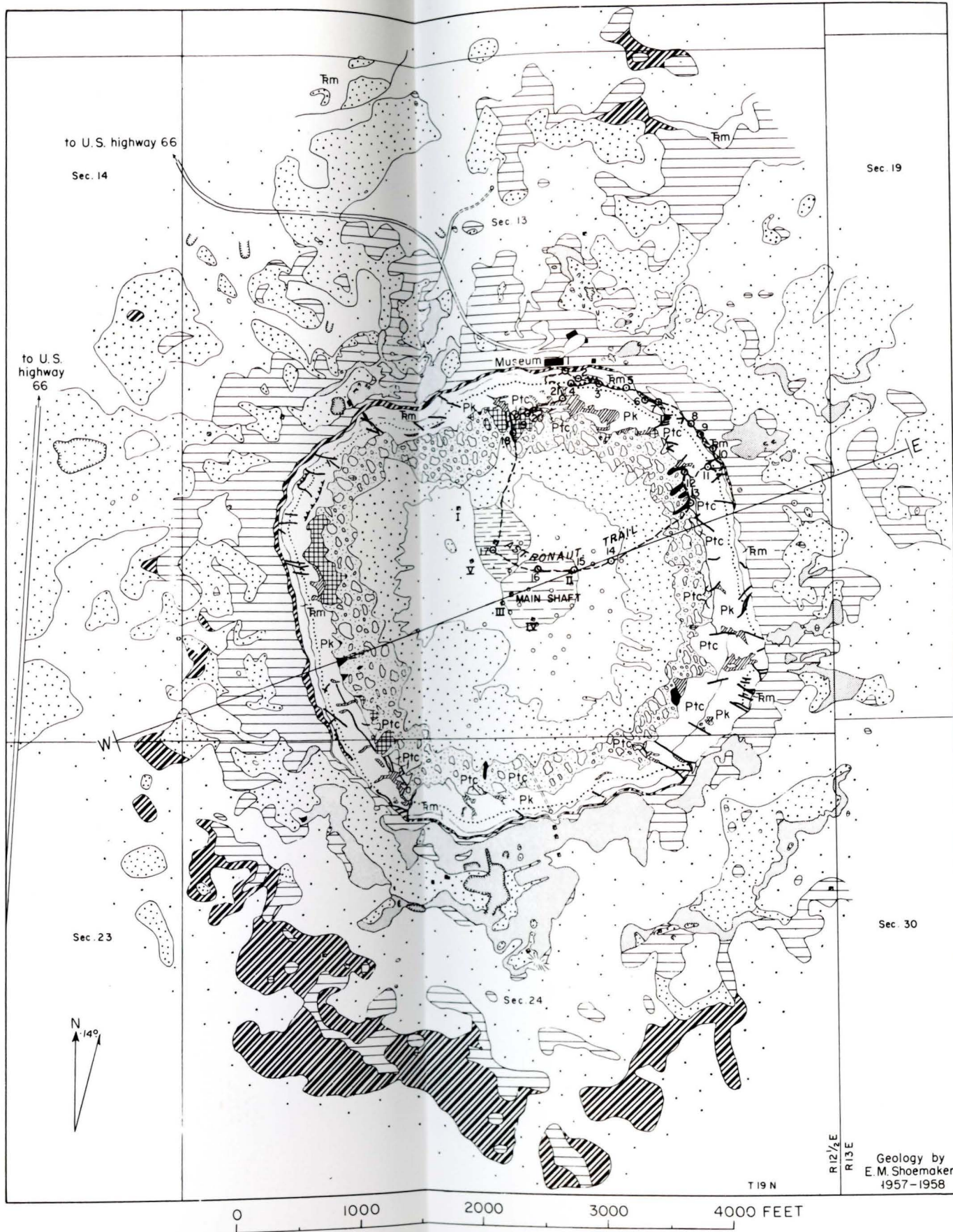
REFERENCES CITED

Baker, A. A., and Reeside, Jr., J. B., 1929, Correlation of the Permian
    of Southern Utah, northern Arizona, northwestern New Mexico, and
    southwestern Colorado: Bull. Amer. Assoc. Petrol. Geol., v. XIII,
    p. 1413-1448.

Barringer, D. M., 1905, Coon Mountain and its crater: Acad. Nat. Sciences,
    Philadelphia Proc., v. 57, p. 861-886.

Barringer, D. M., 1910, Meteor Crater (formerly called Coon Mountain or
    Coon Butte) in northern central Arizona: Published by the author, 24 p.

Barringer, D. M., 1914, Further notes on Meteor Crater, Arizona: Acad.
    Nat. Sciences Philadelphia Proc., v. 66, p. 556-565.

Barringer, D. M., 1924, Further notes on Meteor Crater in northern central
    Arizona (No. 2): Acad. Nat. Sciences Philadelphia Proc., v. 76,
    p. 275-278.

Chao, E.C.T., 1967, Shock effects in certain rock-forming minerals:
    Science, v. 156, p. 192-202.

Chao, E.C.T., Fahey, J. J., Littler, Janet, and Milton, D. J., 1962,
    Stishovite, SiO_2, A very high pressure new mineral from Meteor
    Crater, Arizona: Jour. Geophys. Res., v. 67, p. 419-421.

Chao, E.C.T., Shoemaker, E. M., and Madsen, B. M., 1960, First natural
    occurrence of coesite: Science, v. 132, p. 220.

Colton, H. S. (revised 1967), the basaltic cinder cones and lava flows
    of the San Francisco Mountain volcanic field: Mus. of Northern
    Arizona Bull. No. 10, Northland Press, Flagstaff, Ariz., 58 p.

Damon, P. E., 1965, Correlation and chronology of ore deposits and vol-
    canic rocks: Ann. Prog. Rept., COO-689-50 Contract AT(11-1)-689,
    U.S. Atomic Energy Comm., p. 36-43.

Damon, P. E., Shafigullah, M., and Leventhal, J. S., 1974, K-Ar chronology
    for the San Francisco volcanic field and rate of erosion of the Little
    Colorado, in Geology of Northern Arizona for the Geological Society
    of America, Rocky Mt. Section Meeting, Flagstaff, Arizona, pt. I,
    p. 221.

Darton, N. H., 1910, A reconnaissance of parts of northwestern New Mexico
    and northern Arizona: U.S. Geol. Survey Bull. 435, p. 21.

Fairchild, H. L., 1907, Origin of Meteor Crater (Coon Butte), Arizona:
    Bull. Geol. Soc. America, v. 18, p. 493-504.

Hack, J. T., 1942, The changing physical environment of the Hopi Indians: Peabody Museum Nat. History Papers, v. 35, p. 3-85.

Hager, Dorsey, 1953, Crater mound (Meteor Crater), Arizona, a geologic feature: Am. Assoc. Petroleum Geologists Bull., v. 37, p. 821-857.

Johnson, G. W., 1959, Mineral resource development by the use of nuclear explosives: Calif. Univ., Lawrence Radiation Lab. Rept. 5458, 18 p.

Kennedy, G. C., Wasserburg, G. J., Heard, H. C., and Newton, R. C., 1962, The upper Millphase region in the system SiO_2-H_2O, Am. Jour. Sci., v. 260, p. 501.

Kieffer, S. W., 1970, 1. Shock metamorphism of the Coconino Sandstone at Meteor Crater, Arizona; 2. The specific heat of solids of geophysical interest, Ph.D. thesis, California Institute of Technology, Pasadena.

Kieffer, S. W., 1971, Shock metamorphism of the Coconino Sandstone at Meteor Crater, Arizona: Jour. Geophys. Res., v. 76, p. 5449.

Kieffer, S. W., Phakey, P. P., Christie, J. M., Shock processes in porous quartz (in prep.)

Kluth, C. F., and Kluth, M. J., 1974, Geology of the Elden Mountain area, in Geology of Northern Arizona for the Geological Society of America, Rocky Mt. Section Meeting, Flagstaff, Arizona, pt. II, p. 521.

Leopold, L. B., and Miller, J. P., 1954: A post-glacial chronology for some alluvial valleys in Wyoming: U.S. Geol. Survey Water-Supply Paper 1261, 90 p.

McKee, E. D., 1933, The Coconino Sandstone--its history and origin, in Contributions to Paleontology: Carnegie Inst. Washington Pub. 440, p. 78-115.

McKee, E. D., 1938, The environment and history of the Toroweap and Kaibab Formations of northern Arizona and southern Utah: Carnegie Inst. Washington Pub. 492, 221 p.

McKee, E. D., 1951, Triassic deposits of the Arizona-New Mexico border area: in New Mexico Geol. Soc. Guidebook, 2nd Field Conf., San Juan Basin, p. 85-92.

McKee, E. D., 1954, Stratigraphy and history of the Moenkopi Formation of Triassic age: Geol. Soc. America Mem. 61, 133 p.

Merrill, G. P., 1907, On a peculiar form of metamorphism in silceous sandstone: U.S. Nat. Mus. Proc., v. 32, p. 547-550.

Merrill, 1908, The Meteor Crater of Canyon Diablo, Arizona: its history, origin, and associated meteoritic irons: Smithsonian Inst. Misc Coll., v. 50, p. 461-498.

Merrill, George Perkins, and Tassin, Wirt, 1907, Contributions to the study of Canyon Diablo meteorites: Smiths. Misc. Col. 50, p. 203-215.

Moore, R. B., Wolfe, E. W., and Ulrich, G. E., 1974, Geology of the eastern and northern parts of the San Francisco volcanic field, Arizona, in Geology of northern Arizona for the Geological Society of America, Rocky Mt. Section Meeting, Flagstaff, Arizona, pt. II, p. 465.

Nininger, H. H., 1949, Oxidation studies at Barringer crater. Metal-center pellets and oxide droplets: Am. Philos. Soc. Yearbook, p. 126-130.

Nininger, H. H., 1951a, Condensation globules at Meteor Crater: Science, v. 113, p. 755-756.

Nininger, H. H., 1951b, A resume of researches at the Arizona meteorite crater: Sci. Monthly, v. 72, p. 75-86.

Nininger, H. H., 1954, Impactite slag at Barringer crater: Am. Jour. Sci., v. 252, p. 277-290.

Nininger, H. H., 1956, Arizona's meteorite crater: Denver, Colo., World Press, Inc., 232 p.

Noble, L. F., 1914, The Shinumo Quadrangle: U.S. Geol. Survey Bull. 549, p. 1-100.

Opdyke, N. D., and Runcorn, S. K., 1960, Wind direction in the western United States in the late Paleozoic: Geol. Soc. America Bull. v. 71, p. 959-971.

Peirce, H. W., 1958, Permian sedimentary rocks of the Black Mesa basin area: New Mexico Geol. Soc. 9th Field Conference, Guidebook of the Black Mesa Basin, Northeastern Ariz., p. 82-87.

Peirce, H. W., and Scurlock, J. R., 1972, Arizona well information: Ariz. Bur. Mines Bull. 185, 195 p.

Read, C. B., 1950, Stratigraphy of the outcropping Permian rocks around the San Juan Basin, in New Mexico Geol. Soc. Guidebook of the San Juan Basin, New Mexico and Colorado, p. 62-66.

Reiche, Parry, An analysis of cross-lamination the Coconino Sandstone: The Jour. of Geology, v. XLVI, no. 7, p. 905-932.

Rinehart, J. S., 1958, Distribution of meteoritic debris about the Arizona meteorite crater: Smithsonian Inst. Contrib. Astrophys., v. 2, p. p. 145-160.

Rogers, A. F., 1928, Natural history of the silica minerals; Am. Mineralogist, v. 13, p. 73-92.

Rogers, A. F., 1930, A unique occurrence of lechatelierite or silica glass: Am. Jour. Sci., 5th Ser., v. 19, p. 195-202.

Schuchert, C., 1918, On the carboniferous of the Grand Canyon of Arizona: Amer. Jour. Sci., v. XLV (4th Ser.), p. 347-361.

Shoemaker, E. M., 1960, Penetration mechanics of high velocity meteorites, illustrated by Meteor Crater, Arizona: Internat. Geol. Con., 21st Session, pt. 18, Copenhagen, p. 418-434.

Shoemaker, E. M., Roach, C. H., and Byers, F. M., Jr., 1962, Diatremes and uranium deposits in the Hopi Buttes, Arizona, in Petrologic Studies, a volume to honor A.F. Buddington: Geol. Soc. America, p. 327-355.

Smiley, T. L., 1958, The geology and dating of Sunset Crater, Flagstaff, Arizona, in Guidebook of the Black Mesa Basin, northeastern Arizona, New Mexico Geol. Soc. 9th Field Conf., p. 186-190.

Spencer, L. J., 1933, Meteoric iron and silica-glass from the meteorite craters of Henbury (central Australia) and Wabar (Arabia): Mineralog. Mag., v. 23, p. 387-404.

Tilghman, B. C., 1906, Coon Butte, Arizona: Acad. Nat. Sciences Philadelphia Proc., v. 57, p. 887-914.

von Engelhardt, W., and Stoffler, D., 1967, Stages of shock metamorphism in crystalline rocks of the Rees Basin, Germany, in French, B., and Short, N., eds., Shock Metamorphism of Natural Minerals, Baltimore Md.

PLATE I

EXPLANATION

Recent

Alluvium   Playa beds

UNCONFORMITY

Alluvium   Lake beds

Talus

UNCONFORMITY

Mixed debris from Coconino,
Toroweap, Kaibab, and
Moenkopi formations; includes
lechatelierite and meteoritic
material

Debris from Coconino sand-
stone and Toroweap formation

Debris from Kaibab
limestone

Debris from Moenkopi
formation

UNCONFORMITY

Ŧm

Moenkopi formation

UNCONFORMITY

Pk

Kaibab limestone;
dotted line is
sandstone bed

Ptc

Toroweap formation
and Coconino sand-
stone

Contact

Faults, nearly vertical
or normal

Thrust fault; teeth are
on side of upper plate

Authigenic breccia;
fragments not mixed;
occurs mostly along faults

Allogenic breccia;
fragments mixed; includes
lechatelierite and meteoritic
material

Shaft

Adit

Pit

Dump

Drill hole

Pleistocene

QUATERNARY

TRIASSIC

PERMIAN

Geology by
E.M.Shoemaker
1957–1958

0   1000   2000   3000   4000 FEET

GEOLOGIC MAP OF METEOR CRATER, ARIZONA

PUBLICATIONS
BY THE CENTER FOR METEORITE STUDIES

Title	Author(s)	Year
1. Researches on Meteorites*	Carleton B. Moore (Editor)	1962
2. Catalog of Meteorites, Arizona State University*	Carleton B. Moore and Charles F. Lewis	1964
3. Terrestrial and Lunar Flux of Large Meteorites Through Solar System History*	William K. Hartmann	1966
4. Xenomalies	Marvin W. Rowe	1967
5. The Petrology of Chondritic Meteorites in the Light of Experimental Studies	John W. Larimer	1967
6. Microtektites and the Origin of the Australasian Tektite Strewn Field	Billy P. Glass	1968
7. The Austenite-Ferrite Transformation (Tables relating the Widmanstatten angles in iron meteorites to the plane of section)*	V. F. Buchwald	1968
8. Accretion of Murray Carbonaceous Chondrite and Implications Regarding Chondrule and Chondrite Formation	Donald P. Elston	1969
9. The Published Papers of H. H. Nininger, Biology and Meteoritics	George A. Boyd (Editor)	1971
10. Catalog of Meteorites in the Collections of Arizona State University	Marilyn L.Karr, Charles F. Lewis and Carleton B. Moore	1970
11. Particle Track Studies and the Origin of Gas-Rich Meteorites	Laurel L. Wilkening	1971
12. Meteors and Meteorites in the Ancient Near East	Judith K. Bjorkman	1973
13. Identification of Meteorites	Carleton B. Moore and Paul P. Sipiera	1975
14. Catalog of Meteorites in the Collections of Arizona State University	Charles F. Lewis and Carleton B. Moore	1976
15. A Checklist of Published References to Barringer Meteorite Crater, Arizona 1891-1970	Diana J. Briley and Carleton B. Moore	1976
16. Meteorites — A Photographic Study of Surface Features, Part 1. Shapes	H. H. Nininger	1977
17. Guidebook to the Geology of Meteor Crater, Arizona	Eugene M. Shoemaker and Susan W. Kieffer	1978

*Out of print.